Gastroenterology 2024;166:178–190

PREVENTION AND EARLY DETECTION

A Circulating Panel of circRNA Biomarkers for the Noninvasive and Early Detection of Pancreatic Ductal Adenocarcinoma

Caiming Xu,[1,2,3] Eunsung Jun,[4] Yoshinaga Okugawa,[5] Yuji Toiyama,[5] Erkut Borazanci,[6] John Bolton,[7] Akinobu Taketomi,[8] Song Cheol Kim,[4] Dong Shang,[2,3] Daniel Von Hoff,[9] Guixin Zhang,[2,3] and Ajay Goel[1,10]

[1]Department of Molecular Diagnostics and Experimental Therapeutics, Beckman Research Institute of City of Hope, Biomedical Research Center, Monrovia, California; [2]Department of General Surgery, The First Affiliated Hospital of Dalian Medical University, Dalian, China; [3]Institute (College) of Integrative Medicine, Dalian Medical University, Dalian, China; [4]Division of Hepatobiliary and Pancreatic Surgery, Department of Surgery, Asan Medical Center, University of Ulsan College of Medicine, Seoul, South Korea; [5]Department of Gastrointestinal and Pediatric Surgery, Division of Reparative Medicine, Institute of Life Sciences, Mie University Graduate School of Medicine, Tsu City, Mie, Japan; [6]HonorHealth Research Institute, Scottsdale, Arizona; [7]Department of Surgery, Ochsner Clinic Foundation, New Orleans, Louisiana; [8]Department of Gastroenterological Surgery I, Graduate School of Medicine, Hokkaido University, Sapporo, Hokkaido, Japan; [9]Translational Genomics Research Institute, Phoenix, Arizona; and [10]City of Hope Comprehensive Cancer Center, Duarte, California

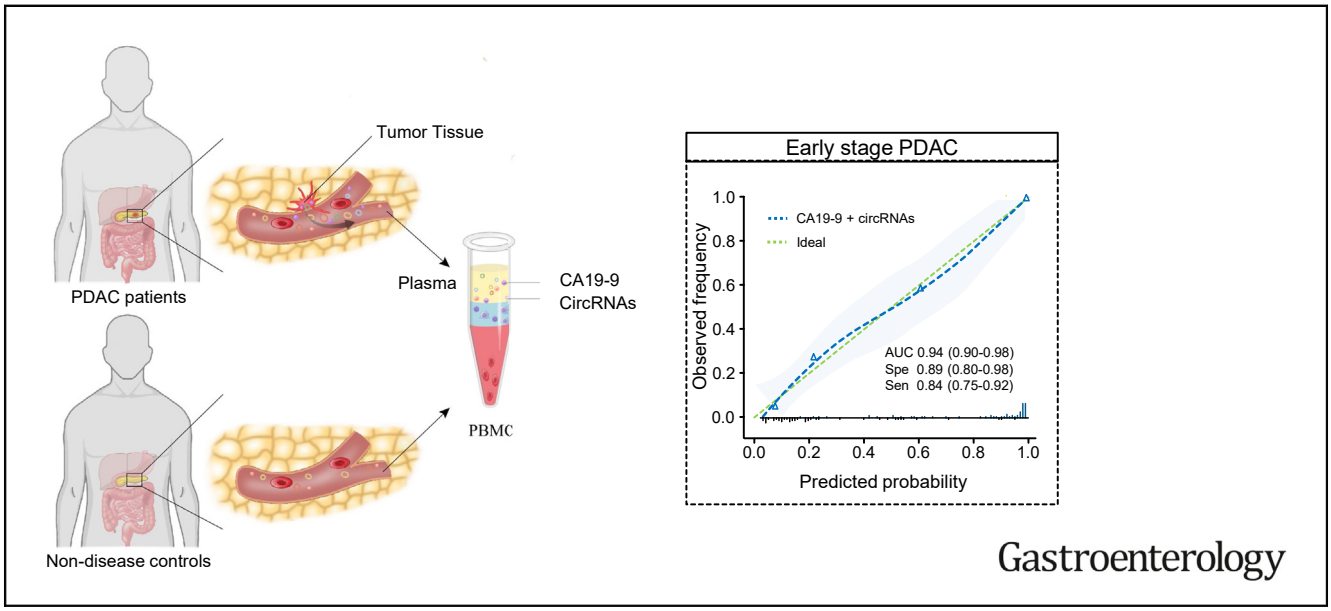

BACKGROUND & AIMS: Pancreatic ductal adenocarcinoma (PDAC) is one of the most fatal malignancies. Delayed manifestation of symptoms and lack of specific diagnostic markers lead patients being diagnosed with PDAC at advanced stages. This study aimed to develop a circular RNA (circRNA)-based biomarker panel to facilitate noninvasive and early detection of PDAC. **METHODS:** A systematic genome-wide discovery of circRNAs overexpressed in patients with PDAC was conducted. Subsequently, validation of the candidate markers in the primary tumors from patients with PDAC was performed, followed by their translation into a plasma-based liquid biopsy assay by analyzing 2 independent clinical cohorts of patients with PDAC and nondisease controls. The performance of the circRNA panel was assessed in conjunction with the plasma levels of cancer antigen 19-9 for the early detection of PDAC. **RESULTS:** Initially, a panel of 10 circRNA candidates was identified during the discovery phase. Subsequently, the panel was reduced to 5 circRNAs in the liquid biopsy–based assay, which robustly identified patients with PDAC and distinguished between early-stage (stage I/II) and late-stage (stage III/IV) disease. The areas under the curve of this diagnostic panel for the detection of early-stage PDAC were 0.83 and 0.81 in the training and validation cohorts, respectively. Moreover, when this panel was combined with cancer antigen 19-9 levels, the diagnostic performance for identifying patients with PDAC improved remarkably (area under the curve, 0.94) for patients in the validation cohort. Furthermore, the circRNA panel could also efficiently identify patients with PDAC (area under the curve, 0.85) who were otherwise deemed clinically cancer antigen 19-9–negative (<37 U/mL). **CONCLUSIONS:** A circRNA-based biomarker panel with a robust noninvasive diagnostic potential for identifying patients with early-stage PDAC was developed.

Keywords: Pancreatic Ductal Adenocarcinoma; Circular RNA; CA19-9; Diagnostic Biomarker; Liquid-Biopsy Assay.

WHAT YOU NEED TO KNOW

BACKGROUND AND CONTEXT

Delayed manifestation of symptoms and the lack of specific diagnostic markers lead to the diagnosis of patients with pancreatic ductal adenocarcinoma (PDAC) at advanced stages when the disease is incurable. This highlights the urgent unmet clinical need to identify and develop diagnostic methods to detect PDAC at its earliest stages.

NEW FINDINGS

We have developed a circular RNA–based biomarker panel that can robustly identify patients with PDAC and performs remarkably well when combined with cancer antigen 19-9.

LIMITATIONS

Our circular RNA diagnostic panel was identified on the basis of case-control studies, and its efficacy in early PDAC detection warrants large-scale cohort validation.

CLINICAL RESEARCH RELEVANCE

Our circular RNA–based panel has the potential to identify patients with PDAC and provides a promising noninvasive approach with high accuracy for the early detection of PDAC combined with cancer antigen 19-9.

BASIC RESEARCH RELEVANCE

The circular RNAs may provide new insights into PDAC tumorigenesis and progression.

Pancreatic cancer (PC) ranks as the fourth leading cause of cancer-associated mortality in the United States, accounting for 8% of all cancer-related deaths in 2022.[1] Among patients with PC, those with pancreatic ductal adenocarcinoma (PDAC) exhibit 5-year survival rates of approximately 12%.[1] One of the primary reasons for the dismal survival rates in PDAC is that most patients are diagnosed at late stages, when the disease is already metastatic. Current estimates indicate that only 10%–15% of patients with PDAC are diagnosed with resectable or borderline resectable disease.[2] These data highlight the urgent unmet clinical need to identify and develop diagnostic methods that could precisely detect PDAC at its earliest stages, when the disease is still confined to within the pancreas and there is still an opportunity for surgical resection of the tumor.

Despite constant improvements in the development of diagnostic imaging technologies, the accuracy of these approaches for the early diagnosis of PDAC remains inadequate.[3] In addition, the most commonly used blood-based biomarker in the clinic, cancer antigen 19-9 (CA19-9), has limited performance in detecting early-stage PDAC. Not only does CA19-9 lack sensitivity as a biomarker for identifying early-stage PDAC, but approximately 50% of patients with pancreatic adenocarcinomas <3 cm in size have elevated CA19-9 levels.[4,5] Furthermore, approximately 10% of patients with PDAC with Lewis antigen–negative blood type are unable to synthesize CA19-9 and will be categorized erroneously as false negative if they were to be diagnosed solely on the basis of circulating levels of this glycoprotein.[6,7] Finally, CA19-9 levels are frequently elevated in other gastrointestinal (GI) malignancies, such as gastric cancer (GC), intrahepatic cholangiocarcinoma, and colorectal cancer (CRC), as well as in benign diseases, such as pancreatitis and obstructive jaundice, limiting its specificity as a diagnostic biomarker for PDAC.[8] Hence, there is an imperative clinical need for developing robust noninvasive biomarkers that could complement CA19-9 for detecting early-stage PDAC.

Circular RNAs (circRNAs) are a class of closed-loop RNAs with a junction between the 3′ and 5′ ends generated by means of splicing their precursor messenger RNAs—a characteristic that makes them more stable than their linear counterparts.[9] CircRNAs are also emerging as important players in the pathogenesis of multiple solid cancers, including PDAC, GC, esophageal squamous cell carcinoma (ESCC), CRC, and hepatocellular cancer (HCC).[10–13] More importantly, recent evidence indicates that circRNAs might have untapped potential as biomarkers for cancer diagnosis and prognosis.[14,15] However, to the best of our knowledge, no study has explored circRNA-based biomarkers for the early detection of PDAC, which was the underlying premise for our study.

We hypothesized that circulating circRNAs might offer diagnostic potential in PDAC. A combination of multiple circRNAs might provide a platform for robust diagnostic performance on their own or in conjunction with CA19-9 levels in the blood. Accordingly, we first undertook a systematic and comprehensive circRNA-based biomarker discovery, followed by the translation of identified candidates into a noninvasive, liquid biopsy–based assay for the early detection of PDAC. These efforts led us to successfully develop a 5-circRNA circulating panel that exhibited robust diagnostic accuracy in PDAC. The performance of these biomarkers was further enhanced when analyzed with CA19-9 for the early detection of this malignancy.

Materials and Methods

Study Design and Patient Cohorts

All participants provided informed written consent and the study protocol was approved by the Institutional Review Board of the University of Ulsan College of Medicine, Ochsner Clinic

Abbreviations used in this paper: **AN, adjacent normal; AUC, area under the curve; CA19-9, cancer antigen 19-9; circRNA, circular RNA; CRC, colorectal cancer; DEC, differentially expressed circular RNA; ESCC, esophageal squamous cell carcinoma; GC, gastric cancer; GI, gastrointestinal; HCC, hepatocellular cancer; NPV, negative predictive value; PC, pancreatic cancer; PDAC, pancreatic ductal adenocarcinoma; PPV, positive predictive value; ROC, receiver operating characteristic; RT-qPCR, real-time quantitative polymerase chain.**

Most current article

0016-5085/$36.00
https://doi.org/10.1053/j.gastro.2023.09.050

Foundation, Mie University Graduate School of Medicine, and Hokkaido University.

The study workflow design is depicted in Supplementary Figure 1. Our study comprised the following 4 phases: a comprehensive circRNA-based biomarker discovery phase, a tissue-based validation phase, a plasma-based training phase, and the final performance evaluation phase in an independent patient cohort.

During the initial biomarker discovery phase, we analyzed genome-wide circRNA expression profiles in 2 independent data sets (GSE69362 and GSE79634) obtained from the Gene Expression Omnibus and based on the same platform GPL19978. The GSE79634 data set included transcriptomic profiling data from 20 primary PDAC tumors and their matched adjacent normal (AN) tissues. The GSE69362 data set included 6 primary PDAC tumors and their matched paracancerous tissues. After the discovery phase, real-time quantitative polymerase chain reaction (RT-qPCR) assays were performed to evaluate the expression of candidate circRNAs in a tissue-based validation cohort consisting of 32 PDAC specimens and an equal number of matched AN specimens from patients enrolled at the Asan Medical Center, Seoul, Korea, between 2012 and 2014. The clinicopathologic characteristics of these 32 PDAC specimens are provided in Supplementary Table 1.[16]

Next, to translate our tissue-based circRNA biomarkers into a liquid biopsy–based assay, we performed qRT-PCR assays for candidate circRNAs in the plasma-based training phase, consisting of 70 patients with PDAC and 35 nondisease controls enrolled at the Asan Medical Center, Seoul, Korea, between 2012 and 2016. Lastly, in the performance evaluation phase, we undertook qRT-PCR assays to quantitatively evaluate the expression of trained circRNAs in an independent cohort of plasma specimens obtained from 88 patients with PDAC, 46 nondisease controls who were enrolled at the Ochsner Clinic Foundation, New Orleans, Louisiana, between 2018 and 2022. The detailed clinical characteristics of plasma training and validation cohorts are provided in Supplementary Table 2.

To assess the specificity of our circRNA-based biomarker panel, we compared its performance in patients with PDAC with several other GI cancers, including ESCC, CRC, GC, and HCC. In these experiments, RT-qPCR assays were applied to examine the expression levels of circRNA markers in 40 patients with each type of GI cancer. Plasma specimens for ESCC and GC were collected from the Nagoya University Hospital (Nagoya, Japan) between 2014 and 2018. For CRC, plasma samples were gathered from patients enrolled at the Mie University Medical Hospital (Mie, Japan) between 2014 and 2016. HCC plasma specimens were enrolled at the Hokkaido University Hospital (Hokkaido, Japan) between 2008 and 2009.

Discovery of circRNA Candidates Using Genome-Wide Expression Profiling

We analyzed circRNA expression profiling data during the biomarker discovery in 2 independent data sets (GSE69362 and GSE79634) to identify differentially expressed circRNA (DEC) associated with PDAC. Such an analysis between PDAC and the matched AN tissues was performed using the R statistical software environment using the "limma" package.[17] The circRNA candidates were initially filtered at a $\log_2$(fold-change) >1 and a P value $<.01$. The top 10 circRNA candidates commonly shared between GSE69362 and GSE79634 data sets sorted using the criteria above were selected for validation in the subsequent phases.

RNA Extraction and Real-Time Quantitative Polymerase Chain Reaction Assays in Tissue and Plasma Specimens

Total RNA was isolated from frozen surgical PDAC specimens, AN pancreatic tissue, and 200 μL of plasma using the RNeasy Mini Kits and miRNeasy Serum/Plasma Kits (Qiagen, Hilden, Germany). The concentration of total cell-free RNA isolated from plasma was quantified using NanoDrop One, and 350 ng total RNA was used for complementary DNA synthesis. The complementary DNA was synthesized using a High-Capacity Reverse Transcription Kit with an RNase inhibitor (Applied Biosystems, Foster City, CA). The RNase-R treatment was used to digest and rule out linear RNA amplification.[18] The resulting RNA was purified using RNeasy MinElute Kit (Qiagen). The expression level of circRNAs was examined by RT-qPCR assays. For all circRNA candidates, the specific divergent primers were designed using the well-established CircInteractome web tool.[19] To ensure the primer specificity for the circRNAs, we designed unique primer sets using the splice-site junctions. The sequences of the primers for each target circRNA are presented in Supplementary Table 3. The RT-qPCR analysis was performed on a QuantStudio 6 flex real-time quantitative PCR system (Applied Biosystems) using a SensiFAST SYBR Lo-ROX Kit (Bioline, London, UK). The β-actin gene was used as an internal control for data normalization. The relative expression values of circRNAs were normalized using the $2^{-\Delta CT}$ method. Log transformation for the fold-change values was performed before further analysis.[15]

Plasma CA19-9 Measurement

The measurement of CA19-9 levels in plasma was performed using the Pancreatic & GI Cancer (Mucin PC/CA199) ELISA Kit (cat. no. 1840; Alpha Diagnostic International, San Antonio, TX), per manufacturer's instructions.

Statistical Analysis

All statistical analyses were performed within the R statistical software environment, version 4.1.2 and GraphPad Prism, version 9.0.2. The DEC analysis between PDAC and the matched AN tissue was performed using the "limma" package. Volcano plots and heatmaps used to visualize the DEC between different groups were plotted based on the "ggplot2" and "pheatmap" packages. The binary logistic regression was performed using the "glm" function of the "DAAG" package. The receiver operating characteristic (ROC) curves were constructed to evaluate the performance of the diagnostic biomarkers using the "pROC" package.[20] The optimal cutoff points for ROC curves were determined using Youden's index in the "pROC" package.[20] The area under the curve (AUC) value, accuracy, sensitivity, specificity, positive predictive value (PPV), negative predictive value (NPV), and precision of circRNAs were calculated across all of the cohorts using the "pROC" package.[20] Decision curve analyses were applied to delineate the net benefit value of the circRNAs for detecting PDAC using the "rmda" package. Calibration curves were developed to assess the calibration of the circRNAs using the "CalibrationCurves" package. Mann-Whitney U test and t test compared 2 independent groups with continuous variables. $P <$ .05 was considered statistically significant.

Results

Genome-Wide Profiling Identified a Panel of 10 circRNAs That Distinguished Pancreatic Ductal Adenocarcinoma From Adjacent Normal Tissue Specimens

The primary objective of this study was to identify circRNAs as biomarkers for detecting patients with PDAC, especially those with early-stage disease. Toward this goal, during the biomarker discovery phase, we first performed a rigorous bioinformatic and statistical analysis to identify candidate circRNAs that were differentially expressed between primary tumors and matched AN tissues in 2 independent data sets of circRNA expression profiling. Based on the DEC analysis, we initially identified a panel of 125 up-regulated and 156 down-regulated circRNAs that discriminated PDAC tissues from the matched AN tissues ($\log_2$ fold-change >1 and $P < .01$) in the GSE79634 data set (Figure 1*A*) and 75 up-regulated and 26 down-regulated circRNAs in the GSE69362 data set (Figure 1*B*), respectively. To develop a circRNA-based diagnostic biomarker panel, using statistical analysis, we prioritized the top 10 overlapping DECs between the 2 data sets that were significantly up-regulated in patients with PDAC (Figure 1*C*, Supplementary Figure 2*A*). Subsequently, we established a logistic regression model and calculated the risk score using the coefficients derived from each of the 10 circRNAs in the training cohort (GSE79634). After that, the ROC analysis was performed to determine the performance of the combined 10-circRNA–based panel for its ability to discriminate PDAC from AN tissues. This analysis revealed that our circRNA biomarker panel robustly distinguished PDAC from the AN tissues with an AUC value of 1.00 (95% CI, 1.00–1.00) and 0.94 (95% CI, 0.82–1.00) in the training (GSE79634, Figure 1*D*) and validation cohorts (GSE69362, Supplementary Figure 2*B*), respectively. These data highlighted that circRNA expression profiling allowed for successful identification of a 10-circRNA panel in 2 independent data sets, which could eventually lead to the translation of these biomarkers into a noninvasive assay for the early detection of patients with PDAC.

Establishment of circRNA–Specific Polymerase Chain Reaction Assays and Validation of Prioritized circRNA Biomarkers in Tissue Specimens From Patients With Pancreatic Ductal Adenocarcinoma

Before validating the identified tissue-based circRNA candidates in plasma specimens, we wanted to ensure that these markers performed robustly in the tissue specimens using the RT-qPCR assays. For preparing RNA for the PCR assays, we first performed the digestion of extracted RNA using the RNase-R enzyme to remove linear RNAs and ensure the specific amplification of circRNAs. Our results indicated that all 10 circRNAs were successfully amplified using the circRNA-specific divergent primers. Subsequently, we evaluated the expression levels of these circRNAs in a subset of 32 paired PDAC and AN tissue specimens. These experiments allowed us to select a panel of 7 circRNAs for further validation, as these were significantly up-regulated in paired PDAC tissues, which was consistent with the discovery phase analyses (Supplementary Figure 3). The expression data [$\log10(2^{-\Delta CT})$] of these 7 circRNAs in the tissue-based validation phase are summarized in Supplementary Table 4. The diagnostic performance of each circRNA candidate regarding their AUC value, diagnostic accuracy, NPV, PPV, sensitivity, and specificity are summarized in Supplementary Table 5.

We next performed logistic regression analysis to calculate the risk score based on the following logit formula: 19.566 + 0.347 × hsa_circ_0060733 + 0.538 × hsa_circ_0007895 – 8.349 × hsa_circ_0064288 + 5.546 × hsa_circ_0006117 + 7.495 × hsa_circ_0007367 + 3.79 × hsa_circ_0066147 – 0.3248 × hsa_circ_0079440. It was noteworthy to observe that although the diagnostic performance of individual circRNA biomarkers was remarkable (Supplementary Table 5), a model comprising all circRNAs exhibited a significantly superior diagnostic performance for the early detection of patients with PDAC (AUC, 0.97; specificity, 0.97; sensitivity, 0.91; accuracy, 0.94) (Figure 2*A*). Subsequently, waterfall plot analysis was performed to dichotomize the cases on the basis of their risk scores. It was encouraging that our model could robustly discriminate between PDAC and AN tissues, with 31 of 34 patients (91.2%) categorized as true positives and 29 of 30 patients (96.7%) categorized as true negatives (Figure 2*B*). Collectively, these data highlighted the significance of our biomarker discovery efforts and successful primer design for amplifying circRNAs and validating a panel of 7 markers for the robust identification of patients with PDAC.

Clinical Translation of the Tissue-Based circRNAs Into a Liquid Biopsy–Based Assay in a Training Cohort of Patients With Pancreatic Ductal Adenocarcinoma

Liquid biopsies have multiple advantages over tissue-based traditional biopsies, including their noninvasiveness, ease of sample collection, and effective detection, which could be exploited as an important tool in the early detection of cancers and patient management.[21,22] Accordingly, we explored the feasibility of translating our tissue-based circRNA panel into a liquid biopsy–based assay in a training cohort of 70 patients with PDAC and 35 nondisease controls. We performed RT-qPCR assays to interrogate the expression levels of the 7 circRNAs in plasma specimens from this training cohort. We noted that the expression levels of hsa_circ_0079440 and hsa_circ_0066147 were extremely low or undetectable in the plasma specimens. Accordingly, we excluded these 2 markers and the remaining 5 circRNAs were selected for further analysis and the liquid biopsy panel development. The expression data [$\log10(2^{-\Delta CT})$] for these 5 circRNA biomarkers in the plasma-based training phase are presented in Supplementary Table 6. To determine the diagnostic performance of individual circRNAs, univariate logistic analysis was performed. The results indicated that all 5 circRNAs exhibited a significant diagnostic performance in identifying patients with PDAC (Supplementary Table 7). The diagnostic performance of each circRNA candidate in terms of

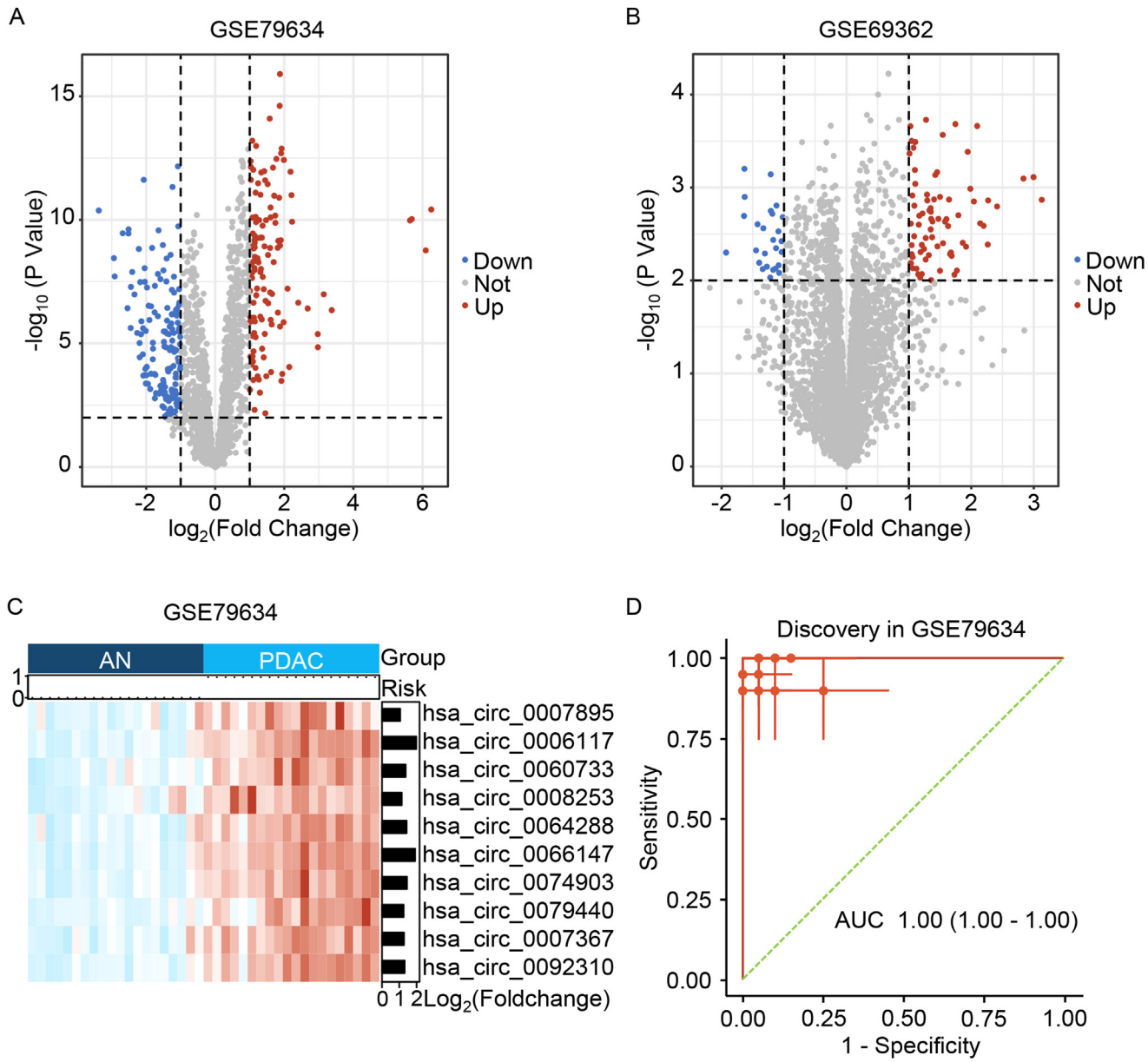

Figure 1. Genome-wide discovery of circRNA candidates for PDAC diagnosis. *Volcano plots* illustrate the $\log_2$ fold-change and the corresponding *P* values for DECs in 2 independent circRNA expression data sets: GSE79634 (*A*) and GSE69362 (*B*). $P < .01$ was considered statistically significant. (*C*) The *heatmap* depicts the top 10 overlapping up-regulated circRNAs (sorted by *P* value) among the patients with PDAC (n = 20) and matched AN tissues (n = 20) in the discovery data set (GSE79634). (*D*) ROC curve analysis shows the performance of the 10-circRNA panel. *Red lines* indicate the specificity and sensitivity with 95% CIs for each circRNA under the best threshold; *red points* indicate the optimal threshold for specificity and sensitivity.

their AUC values, diagnostic accuracy, NPV, PPV, sensitivity, and specificity are summarized in Supplementary Table 8. After that, we calculated the risk score for each case on the basis of the coefficients generated from logistic regression analysis: 1.0468 + 1.294 × hsa_circ_0060733 + 0.8915 × hsa_circ_0006117 - 0.0867 × hsa_circ_0064288 + 0.6066 × hsa_circ_0007895 + 0.1428 × hsa_circ_0007367. As was the case in the tissue phase, the diagnostic performance of the combination panel of 5-circRNA biomarkers demonstrated a markedly better diagnostic performance vis-à-vis individual circRNA biomarkers (AUC, 0.83; specificity, 0.74; sensitivity, 0.89; accuracy, 0.84) (Figure 2*C*). Furthermore, waterfall plot analysis also depicted that the combined circRNA panel successfully discriminated patients with PDAC from the non-disease controls (Figure 2*D*); 62 of 71 cases (87.3%) were true positives and 26 of 34 cases (76.5%) were true negatives.

Successful Validation of the circRNA–Based Liquid Biopsy Assay in an Independent Cohort of Patients With Pancreatic Ductal Adenocarcinoma

Next, we further validated the diagnostic performance of the trained 5-circRNA–based liquid biopsy biomarker panel in an independent cohort comprising 88 patients with PDAC

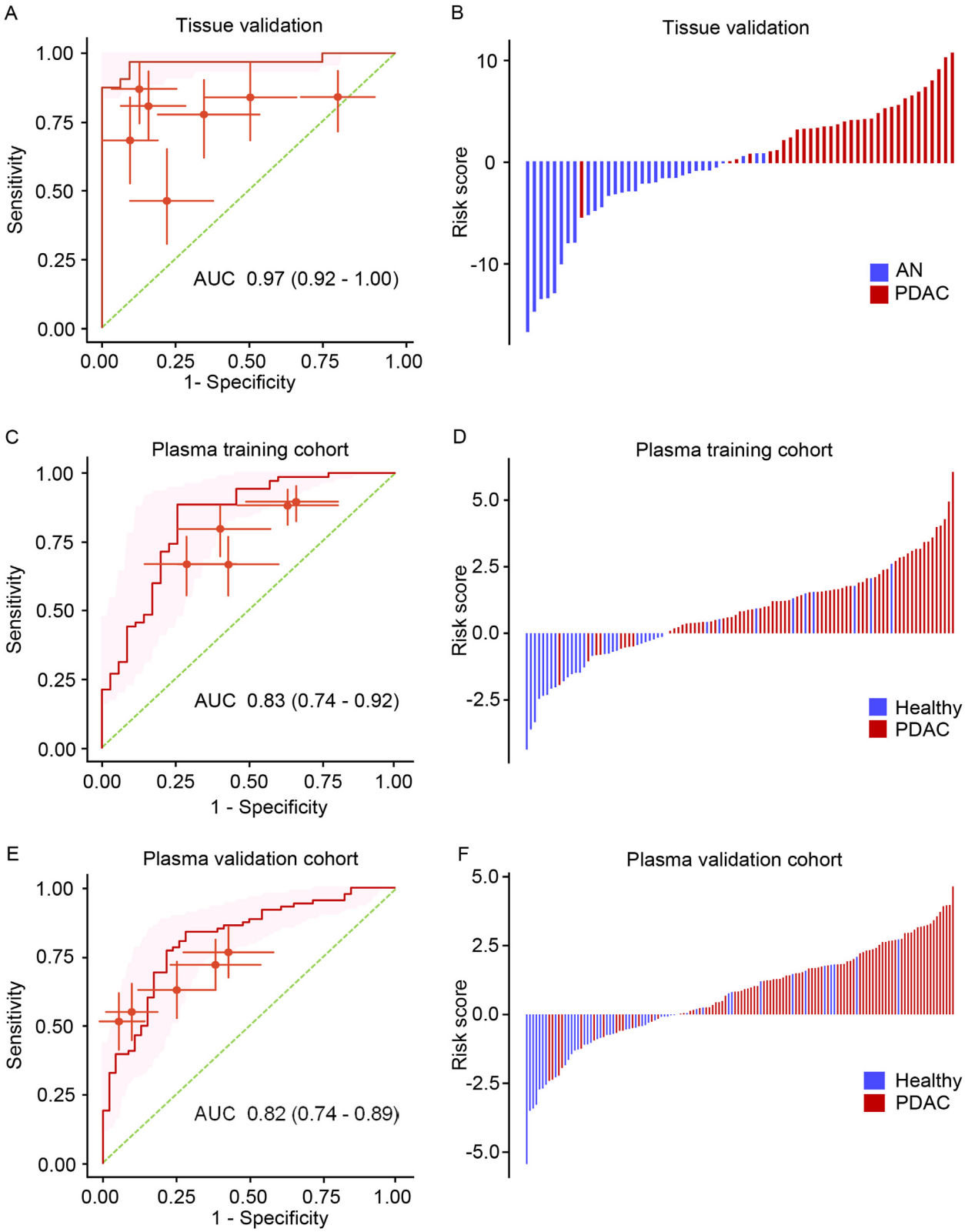

Figure 2. Validation and performance evaluation of the candidate circRNAs in tissue and plasma specimens from clinical cohorts. (*A*) ROC curve analysis reveals the performance of the selected 7-circRNA panel in 32 pairs of PDAC and AN tissues. ROC curves are shown as 95% CIs. *Red lines* indicate the specificity and sensitivity with 95% CI for each circRNA under the best threshold. The *red points* depict the optimal threshold for specificity and sensitivity. (*B*) The *waterfall plot* illustrates the risk probability distribution between matched PDAC and AN tissues. (*C*) ROC curve analysis reveals the diagnostic potential of the final 5-circRNA panel in the training cohort. (*D*) The *waterfall plot* illustrates the risk probability distribution between plasma samples of patients with PDAC (n = 70) and the nondisease controls (n = 35) in the training cohort. (*E*) ROC curve analysis reveals the performance of the 5-circRNA panel in the validation cohort. (*F*) The *waterfall plot* illustrates the risk probability distribution between patients with PDAC (n = 88) and nondisease controls (n = 46) in the validation cohort.

Table 1. Summary of the Diagnostic Performance of Individual circRNAs in the Performance Evaluation Cohort

circRNA ID	AUC (95% CI)	Accuracy (95% CI)	PPV (95% CI)	Sensitivity (95% CI)	Specificity (95% CI)	NPV (95% CI)
hsa_circ_0060733	0.72 (0.63–0.81)	0.66 (0.59–0.75)	0.82 (0.75–0.90)	0.63 (0.52–0.73)	0.74 (0.61–0.87)	0.51 (0.43–0.60)
hsa_circ_0006117	0.72 (0.63–0.80)	0.66 (0.59–0.74)	0.91 (0.83–0.98)	0.55 (0.43–0.65)	0.89 (0.80–0.98)	0.51 (0.45–0.58)
hsa_circ_0064288	0.72 (0.63–0.80)	0.69 (0.61–0.77)	0.77 (0.71–0.83)	0.76 (0.66–0.85)	0.57 (0.43–0.70)	0.56 (0.44–0.67)
hsa_circ_0007895	0.75 (0.67–0.83)	0.66 (0.58–0.73)	0.94 (0.87–1.00)	0.51 (0.41–0.61)	0.93 (0.85–1.00)	0.50 (0.45–0.56)
hsa_circ_0007367	0.66 (0.56–0.76)	0.68 (0.60–0.76)	0.78 (0.71–0.85)	0.72 (0.61–0.81)	0.61 (0.46–0.74)	0.53 (0.43–0.64)

and 46 nondisease controls. The RT-qPCR assays were performed to interrogate the expression levels of each of the 5 circRNAs in plasma samples (Supplementary Table 9). The diagnostic performance of each circRNA candidate in terms of their AUC values, diagnostic accuracy, NPV, PPV, sensitivity, and specificity are summarized in Table 1. After that, using the same diagnostic formula and statistical correlates established in the training cohort, the risk scores for each patient with PDAC were calculated in the validation cohort. Consistent with our results from the training set, ROC analysis suggested the robust ability of the circRNA panel to distinguish patients with PDAC from nondisease controls with an AUC value of 0.82 (95% CI, 0.74–0.89), a sensitivity of 0.84, and with a corresponding specificity of 0.71 (Figure 2*E*). All patients with PDAC were further dichotomized on the basis of the cutoff value of the risk probability (Youden's index). The waterfall plot analysis was performed to represent the diagnostic potential of the validated circRNA panel (Figure 2*F*), which revealed that 74 of 87 cases (85.1%) were true positives and 33 of 47 cases (70.2%) were true negatives. These results highlighted that the 5-circRNA liquid biopsy panel has the clinical potential for use as a noninvasive assay for the early detection of patients with PDAC.

The Noninvasive circRNA Panel Robustly Identifies Patients With Pancreatic Ductal Adenocarcinoma at the Earliest Disease Stages

In PDAC, given the challenges associated with surgical resection of the diagnosed cancer, it is imperative to identify the disease at its earliest stages to improve the surgical resection rate and render a favorable prognosis. When we segregated all patients with PDAC into early (stages I and II) and late stages (stages III and IV), we observed that the risk scores derived from our circRNA markers were relatively high in both groups of patients with PDAC compared with the nondisease controls (Figure 3*A*). More importantly, we did not observe any significant difference in the risk scores between the early- and late-stage patients, indicating that our circRNA-based panel was equally robust in the identification of patients with PDAC, even at the earliest stages (Figure 3*A*). Therefore, we next systematically examined the diagnostic potential of the circRNA panel in the patients with early-stage PDAC, which yielded a remarkable AUC value of 0.83 (specificity, 0.74; sensitivity, 0.90; accuracy, 0.83) in the training cohort (Figure 3*B*) and an AUC value of 0.81 (specificity, 0.72; sensitivity, 0.83; accuracy, 0.78), in the validation cohort (Figure 3*C*). These results highlight the clinical significance of our circRNA-based transcriptomic assay, which performs robustly in the earliest stages of PDAC, offering a potential biomarker option for clinical translation for the noninvasive identification of patients with early-stage PDAC.

The circRNA Panel Is More Specific for Patients With Pancreatic Ductal Adenocarcinoma Than Those With Other Gastrointestinal Cancers

For any blood-based liquid biopsy assay, it is essential to determine whether the prioritized biomarkers performed robustly for the intended tumor type vs other cancers. Therefore, to evaluate the specificity of the 5-circRNA panel for PDAC, we compared its diagnostic performance in patients with several other GI cancers, including ESCC, CRC, GC, HCC, and nondisease controls. It was intriguing to observe that our 5-circRNA panel had the highest diagnostic performance for identifying patients with PDAC (AUC, 0.83) compared with all of the other GI cancers (ESCC: AUC, 0.71; CRC: AUC, 0.69; GC: AUC, 0.58; and HCC: AUC, 0.54; Figure 3D), highlighting the cancer specificity of the circRNA biomarkers for the early detection of patients with PDAC.

Combining the circRNA–Based Panel With CA19-9 Improves Its Performance for the Early Detection of Pancreatic Ductal Adenocarcinoma

Finally, we asked whether the inclusion of the most prevalently analyzed serologic tumor marker in patients with PDAC, the CA19-9 glycoprotein, might further improve the overall diagnostic performance of our circRNA panel. For these experiments, we first examined the plasma CA19-9 levels in patients with PDAC enrolled in the validation cohort. The ROC analysis examined the diagnostic performance of CA19-9 in PDAC with an AUC value of 0.87 (specificity, 0.89; sensitivity, 0.77) (Figure 4*A*). More importantly, the diagnostic performance was significantly increased when we combined the circRNA panel with CA19-9 levels, which yielded an AUC value of 0.95 (specificity, 0.96; sensitivity, 0.82) (Figure 4*A*). These results highlight that CA19-9 can robustly improve the diagnostic

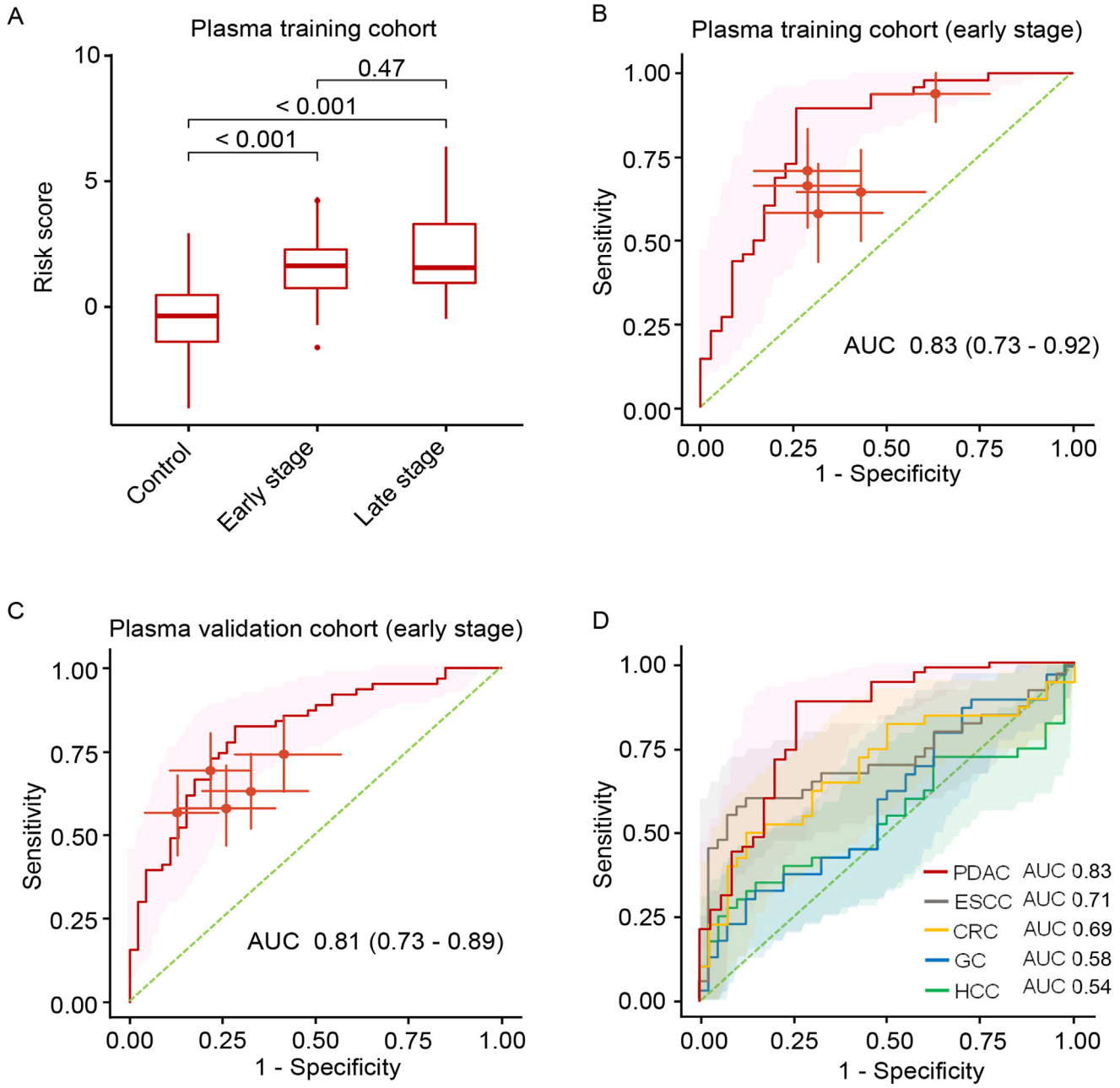

Figure 3. Performance evaluation of the developed circRNA panel to identify patients with early-stage PDAC. (*A*) The circRNA-based risk score was analyzed in patients with PDAC with early and advanced stages from the training cohort. (*B*) ROC curve analysis demonstrates the 5-circRNA panel's performance and the risk probability distribution between the plasma samples of the patients with PDAC (n = 48) and nondisease controls (n = 35) in the training cohort. (*C*) ROC curve analysis demonstrates the 5-circRNA panel's performance and the risk probability distribution between the plasma samples of the patients with PDAC (n = 63) and nondisease controls (n = 46) in the validation cohort. ROC curves are shown as 95% CI. *Red lines* indicate the specificity and sensitivity with 95% CI for each circRNA under the best threshold. *Red points* indicate the sensitivity and specificity with 95% CI for each circRNA under the best threshold. (*D*) ROC curve analysis reveals the performance of the 5 circRNA biomarker–based risk score in different GI malignancies (ie, ESCC, CRC, GC, and HCC).

performance of the circRNA panel for early detection of patients with PDAC.

Interestingly, in our validating cohort, there were 20 patients with PDAC with a CA19-9 level <37 U/mL, a cutoff threshold below which individuals are generally considered negative for PDAC in clinical settings. Herein, we interrogated the circRNA panel's ability to diagnose PDAC in this group of CA19-9–negative cases (20 patients with PDAC and 41 nondisease controls, the detailed clinical characteristics are provided in Supplementary Table 10). Consistent with our previous findings, the circRNA assay exhibited a robust diagnostic performance with an AUC value of 0.85 (specificity, 0.76; sensitivity, 0.85; Figure 4*B*). It is noteworthy that our circRNA panel had a high sensitivity, which might

be conducive to reduce omission diagnosis for early-stage PDAC. We then compared the expression levels of CA19-9 in patients with early- and late-stage PDAC from the validation cohort (Figure 4*C*). We found that the expression of CA19-9 was significantly higher in late-stage patients than in early-stage patients. However, there were no

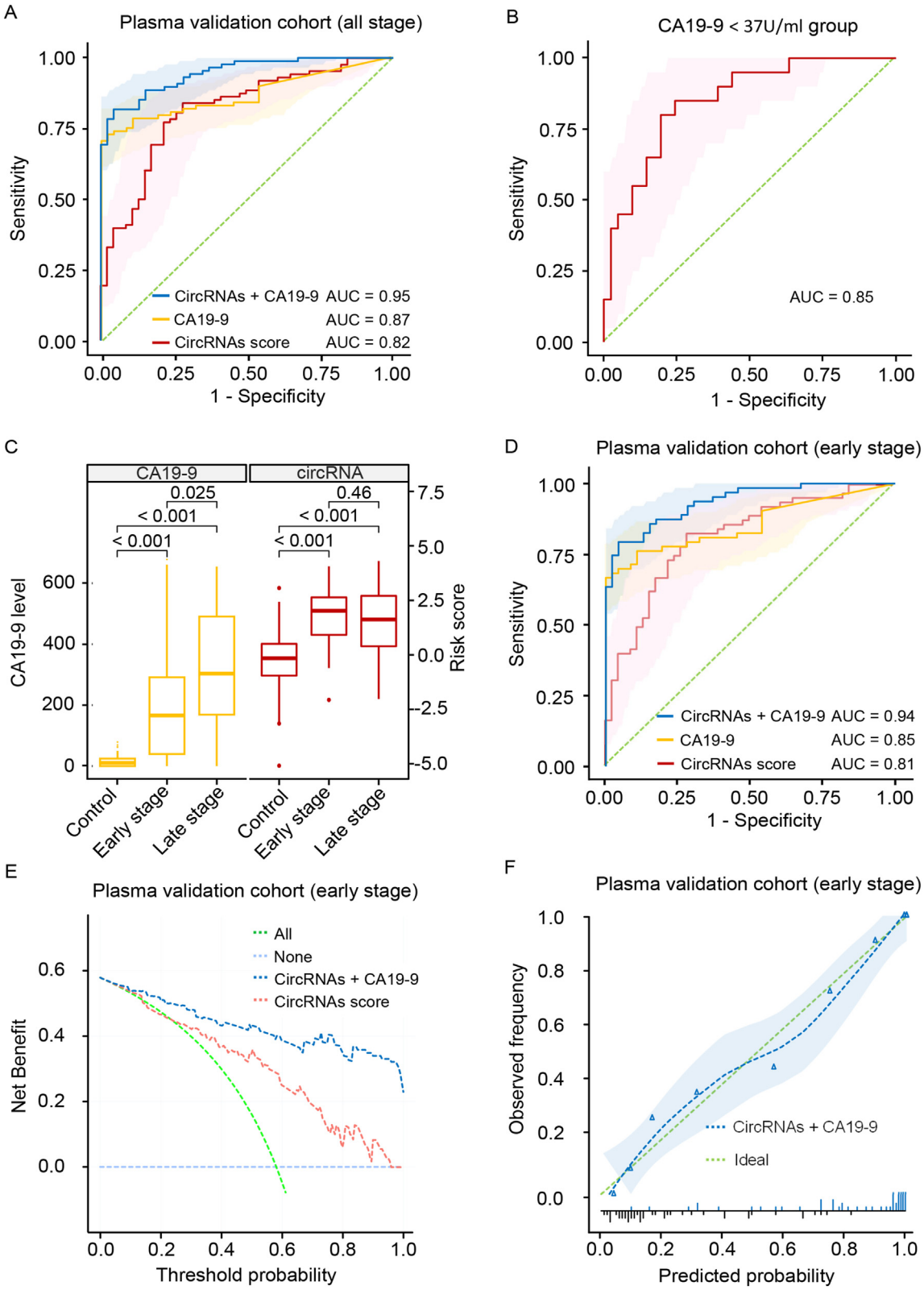

Table 2. The Diagnostic Performance of CA19-9 Alone and circRNA Panel in Combination With CA19-9 at Varying Specificity Thresholds

Variable	Stages	Controls, n	PDAC, n	AUC (95% CI)	Sensitivity (95% CI)	Sens@95%Spec (95% CI)	Sens@97.5%Spec (95% CI)
CA19-9	All stages	46	88	0.87 (0.80–0.93)	0.77 (0.69–0.85)	0.74 (0.64–0.83)	0.72 (0.63–0.82)
CircRNA + CA19-9	All stages	46	88	0.95 (0.91–0.98)	0.82 (0.73–0.90)	0.81 (0.67–0.90)	0.78 (0.63–0.89)
CA19-9	Early stages	46	63	0.85 (0.78–0.93)	0.74 (0.63–0.84)	0.70 (0.57–0.82)	0.68 (0.57–0.81)
CircRNA + CA19-9	Early stages	46	63	0.94 (0.89–0.98)	0.79 (0.68–0.89)	0.77 (0.60–0.89)	0.75 (0.56–0.87)

Sens@95%Spec, sensitivity after fixing the specificity at 95%; Sens@97.5%Spec, sensitivity after fixing the specificity at 97.5%.

significant differences in expression of circRNAs between early- and late-stage PDAC, which was consistent with the results observed in the training cohort (Figure 4*C*). These results suggest that the circRNA panel might help overcome the diagnostic limitations of CA19-9 as a tumor marker with low sensitivity in early-stage diagnosis. Therefore, we examined the diagnostic capacity of the circRNA panel combined with CA19-9 in early-stage PDAC by ROC analysis (AUC, 0.94; specificity, 0.96; sensitivity, 0.79; accuracy, 0.86) (Figure 4*D*).

The decision curve analysis indicated that the circRNA panel combined with CA19-9 offered a superior net benefit vs the circRNA panel in the validation cohort across most ranges of threshold probability in the validation set for diagnosis of early-stage of PDAC (Figure 4*E*). For instance, at a threshold probability of 43% (a recommended threshold value for diagnostic ascertainment of suspicious pancreatic mass),[23] the circRNA panel combined with CA19-9 exhibited a significantly higher net benefit of 0.46 for the diagnosis of PDAC compared with that of circRNA panel with a net benefit of approximately 0.35. Furthermore, the favorable calibration also confirmed that the predicted probability of circRNA and CA19-9 combination matched the actual probability of early-stage PDAC in the validation set (Figure 4*F*), and the Hosmer-Lemeshow test suggested that there was no separation from the ideal fit ($\chi^2 = 2.34$; degrees of freedom = 8; $P = .97$).

Next, the diagnostic performances of CA19-9 and circRNA combined with CA19-9 levels were explored after locking down the assay's specificity at 95% and 97.5%, respectively. In the case of CA19-9 levels alone at a fixed specificity of 95% and 97.5%, a significantly lower sensitivity of 74% and 72% in all stages of patients with PDAC and 70% and 68% in patients with early-stage PDAC, respectively. However, combining the final transcriptomic signature with CA19-9 levels yielded a remarkably higher sensitivity of 81% and 78% for all stages of patients with PDAC and a sensitivity of 77% and 75% in patients, even in patients with early-stage PDAC (Table 2). These results again demonstrate that our circRNA-based transcriptomic assay can substantially improve the overall diagnostic accuracy, highlighting its potential translation into the clinic for early detection of patients with PDAC.

Discussion

The overall incidence of PDAC has increased progressively by approximately 1% annually during the past 2 decades, with 64,050 new cases and 50,550 deaths projected to occur in 2023.[1] PDAC is projected to become the second leading cause of cancer-related deaths by 2030.[24] Although the 5-year survival is estimated to be as high as 27%–44% for PDAC cases diagnosed at an early stage (localized disease),[1,25,26] most patients with PDAC are diagnosed at late stages due to the unavailability of robust diagnostic biomarkers and late manifestation of the disease symptoms. Currently, endoscopic ultrasonography, magnetic resonance imaging, magnetic resonance cholangiopancreatography, endoscopic retrograde cholangiopancreatography, and positron emission tomography are used for PC screening in

Figure 4. The combined performance of the circRNA panel and CA19-9 for the identification of patients with PDAC. (*A*) ROC curve analysis reveals the performance of the circRNA panel, CA19-9, and a combination of both for detecting all-stage patients with PDAC in the validation cohort. (*B*) ROC curve analysis reveals the performance of the circRNA panel in patients with CA19-9 levels under the cutoff value (37 U/mL) from the validation cohort. (*C*) The risk score levels of the circRNA panel and CA19-9 in nondisease controls, patients with early-stage PDAC, and patients with advanced-stage PDAC from the validation cohort. (*D*) ROC curve analysis reveals the performance of the circRNA panel, CA19-9, and a combination of both in patients with early-stage PDAC from the validation cohort. (*E*) *Decision curve* shows the net benefit curves for the circRNA panel alone and the combined CA19-9 and the circRNA in early-stage patients from the validation cohort. The x-axis indicates the threshold probability for PDAC diagnosis and y-axis indicates the net benefit. The d*otted blue line* indicates a combination of CA19-9 and the circRNA panel. (*F*) Calibration curves of the combination of CA19-9 and the circRNA signature in patients with early-stage PDAC from the validation cohort. The *dashed blue line* is the flexible calibration (loess) of CA19-9 combined with the circRNA signature. The *dashed green line* is the ideal line. The *triangle symbol* indicates the grouped observations. The *short blue line* on the horizontal axis and the *short black line* represent the positive and negative cases, respectively.

high-risk patients.[27,28] However, their adaptation to PDAC screening has been challenging due to the high cost, invasive nature, and low sensitivity for smaller, early-stage lesions. Therefore, noninvasive and highly specific biomarkers for early diagnosis could significantly improve the early identification of asymptomatic high-risk patients with PDAC, eventually leading to a better prognosis.

Emerging evidence indicates that circRNAs are highly stable due to their circular structure and abundant presence in various body fluids, including plasma, saliva, and urine.[14] More importantly, circRNAs possess cell- and tissue-specific expression, making them attractive liquid biopsy–based biomarkers.[29] With this in mind, we developed a circRNA panel to discriminate patients with early-stage PDAC from healthy controls and evaluate its translational potential for the early detection of patients with PDAC.

We first performed a biomarker discovery in 2 circRNA profiling data sets. We identified 10 up-regulated candidates in PDAC vs matched AN tissues and ultimately trained a panel of 7 circRNAs in the tissue-based cohorts for further translation into a liquid biopsy assay. Subsequently, after rigorous training and validation, we successfully constructed a panel of 5 circRNAs in plasma, which robustly distinguished between patients with PDAC, including those with an early-stage disease vs nondisease controls. The 5-circRNA panel exhibited AUCs of 0.83 (95% CI, 0.73–0.92) and 0.81 (95% CI, 0.73–0.89) for identifying patients with early-stage PDAC in the training and validation cohorts, respectively. Furthermore, we confirmed that our 5-circRNA panel was PDAC-specific and possessed the highest AUC values vs other GI cancers. The AUC of our 5-circRNA panel for identifying other GI cancers also suggested that this circRNA panel might also have the potential to serve as an early detection assay for patients with ESCC and CRC; however, additional studies are warranted to confirm these findings. To further study the complementarity of the 5-circRNA panel in combination with CA19-9, we evaluated the combined diagnostic potential of these 2 biomarkers in all stages of PDAC, including early stages, as well as in patients who were deemed CA19-9–negative clinically (<37 U/mL).[30] The circRNA-based panel combined with CA19-9 improved the overall diagnostic performance for patients with PDAC at different stages, yielding an AUC value of 0.95 (95% CI, 0.91–0.98) and 0.94 (95% CI, 0.89–0.98) for the detection of all stages and early-stage PDAC, respectively, in the validation cohort. In addition, the 5-circRNA panel displayed an AUC value of 0.85 (95% CI, 0.76–0.95) for identifying CA19-9–negative patients with PDAC, which is clinically significant and highlights the superiority of our circRNA markers over the classical tumor marker. Although there is a risk of producing false-positive cases using our circRNA combined with CA19-9, this integrated panel could identify more high-risk individuals for further investigation using other tests, including endoscopic ultrasonography, magnetic resonance cholangiopancreatography, and endoscopic retrograde cholangiopancreatography.

As for the biological function of the circRNAs in our panel, we observed that most of the identified circRNAs were previously found to play essential roles in tumorigenesis and cancer development. For instance, hsa_circ_0007367 was reported to act as a competing endogenous RNA for promoting disease progression in multiple solid cancers.[31,32] In addition, hsa_circ_0006117 has been linked to facilitating the progression of PC by regulating the miR-96-5p/KRAS/MAPK pathway.[33] Likewise, the hsa_circ_0007895 induces energy production via ATP synthesis to promote PDAC progression through the miR-1294/c-Myc axis.[34] Zhu et al[35] established the competitive endogenous RNA regulatory network consisting of circRNA (including 5 circRNAs in our panel)–microRNA–messenger RNA and predicted the potential regulatory mechanisms of tumorigenesis in PDAC.

We would like to acknowledge some of the potential limitations of our study. First, we included only the circRNA biomarkers that were significantly up-regulated in patients with PDAC vs controls, which would facilitate a more straightforward translation of our assay in the clinical settings. However, it is important to acknowledge that this approach might lead to the omission of down-regulated candidates, which may have other potential biological or clinical implications. Second, although the current results are based on PDAC cases with definite disease status, these data do not suggest the clinical performance of our markers in a prediagnostic setting. Furthermore, the nondisease control cohorts comprised slightly more female subjects and a somewhat younger population than patients with PDAC. To avoid this potential confounder, future studies that include gender- and age-matched nondisease control subjects are needed to further confirm the diagnostic performance of our reported biomarkers. Moreover, all of the PDAC plasma samples were collected at diagnosis; therefore, it needs to be clarified how this 5-circRNA panel might perform in patients after surgical resection. The expression of these circRNAs in patients after surgical resection is expected to be similar to nondisease controls once the tumor is excised successfully. In contrast, their expression would rise again if the patient experiences tumor recurrence later in life. Furthermore, because the circRNA signature was constructed based on case-control studies, we may only know how it will work in surveillance once risk-strategic, well-designed, and large prospective validation studies are conducted. Although the performance seems promising, further investigation is warranted for our circRNA-based panel of biomarkers to be found eligible as a reliable clinical test.

In summary, we reported the identification and validation of a circRNA-based panel for the early detection of patients with PDAC, which was trained and validated in multiple independent cohorts of patients and controls. More importantly, the diagnostic performance of our 5-circRNA panel was further improved when combined with CA19-9 levels, which is attractive, given that this tumor marker is routinely analyzed in a clinical setting. Finally, our circRNA markers' ability to identify patients deemed clinically negative for CA19-9 highlights the clinical significance of these noncoding RNA markers as noninvasive and robust markers for the early detection of patients with PDAC.

Supplementary Material

Note: To access the supplementary material accompanying this article, visit the online version of *Gastroenterology* at www.gastrojournal.org, and at http://doi.org/10.1053/j.gastro.2023.09.050.

References

1. Siegel RL, Miller KD, Wagle NS, Jemal A. Cancer statistics, 2023. CA Cancer J Clin 2023;73:17–48.
2. Versteijne E, van Dam JL, Suker M, et al. Neoadjuvant chemoradiotherapy versus upfront surgery for resectable and borderline resectable pancreatic cancer: long-term results of the Dutch randomized PREOPANC trial. J Clin Oncol 2022;40:1220–1230.
3. Toft J, Hadden WJ, Laurence JM, et al. Imaging modalities in the diagnosis of pancreatic adenocarcinoma: a systematic review and meta-analysis of sensitivity, specificity and diagnostic accuracy. Eur J Radiol 2017; 92:17–23.
4. Capello M, Bantis LE, Scelo G, et al. Sequential validation of blood-based protein biomarker candidates for early-stage pancreatic cancer. J Natl Cancer Inst 2017; 109(4):djw266.
5. Scara S, Bottoni P, Scatena R. CA 19-9: biochemical and clinical aspects. Adv Exp Med Biol 2015;867:247–260.
6. Parra-Robert M, Santos VM, Canis SM, et al. Relationship between CA 19.9 and the Lewis phenotype: options to improve diagnostic efficiency. Anticancer Res 2018; 38:5883–5888.
7. Ballehaninna UK, Chamberlain RS. The clinical utility of serum CA 19-9 in the diagnosis, prognosis and management of pancreatic adenocarcinoma: an evidence based appraisal. J Gastrointest Oncol 2012; 3:105–119.
8. Luo G, Jin K, Deng S, et al. Roles of CA19-9 in pancreatic cancer: biomarker, predictor and promoter. Biochim Biophys Acta Rev Cancer 2021;1875:188409.
9. Kristensen LS, Andersen MS, Stagsted LVW, et al. The biogenesis, biology and characterization of circular RNAs. Nat Rev Genet 2019;20:675–691.
10. Wang C, Liu WR, Tan S, et al. Characterization of distinct circular RNA signatures in solid tumors. Mol Cancer 2022;21:63.
11. Kristensen LS, Jakobsen T, Hager H, et al. The emerging roles of circRNAs in cancer and oncology. Nat Rev Clin Oncol 2022;19:188–206.
12. Li F, Yang Q, He AT, et al. Circular RNAs in cancer: limitations in functional studies and diagnostic potential. Semin Cancer Biol 2021;75:49–61.
13. Wong CH, Lou UK, Li Y, et al. CircFOXK2 promotes growth and metastasis of pancreatic ductal adenocarcinoma by complexing with RNA-binding proteins and sponging miR-942. Cancer Res 2020;80:2138–2149.
14. Li S, Han L. Circular RNAs as promising biomarkers in cancer: detection, function, and beyond. Genome Med 2019;11:15.
15. Roy S, Kanda M, Nomura S, et al. Diagnostic efficacy of circular RNAs as noninvasive, liquid biopsy biomarkers for early detection of gastric cancer. Mol Cancer 2022; 21:42.
16. Amin MB, Edge SB, Greene FL, et al. AJCC Cancer Staging Manual. 8th edition. Springer Cham, 2017.
17. Ritchie ME, Phipson B, Wu D, et al. limma powers differential expression analyses for RNA-sequencing and microarray studies. Nucleic Acids Res 2015; 43(7):e47.
18. Zhang J, Chen S, Yang J, et al. Accurate quantification of circular RNAs identifies extensive circular isoform switching events. Nat Commun 2020;11:90.
19. Dudekula DB, Panda AC, Grammatikakis I, et al. CircInteractome: a web tool for exploring circular RNAs and their interacting proteins and microRNAs. RNA Biol 2016; 13:34–42.
20. Robin X, Turck N, Hainard A, et al. pROC: an open-source package for R and S+ to analyze and compare ROC curves. BMC Bioinform 2011;12:77.
21. Raza A, Khan AQ, Inchakalody VP, et al. Dynamic liquid biopsy components as predictive and prognostic biomarkers in colorectal cancer. J Exp Clin Cancer Res 2022;41:99.
22. Shigeyasu K, Toden S, Zumwalt TJ, et al. Emerging role of microRNAs as liquid biopsy biomarkers in gastrointestinal cancers. Clin Cancer Res 2017;23: 2391–2399.
23. Sonnenberg A, Rodriguez SA, Faigel DO. Diagnostic ascertainment of suspicious pancreatic mass: a threshold analysis. Clin Gastroenterol Hepatol 2008; 6:1162–1166.
24. Rahib L, Smith BD, Aizenberg R, et al. Projecting cancer incidence and deaths to 2030: the unexpected burden of thyroid, liver, and pancreas cancers in the United States. Cancer Res 2014;74:2913–2921.
25. Balasenthil S, Huang Y, Liu S, et al. A plasma biomarker panel to identify surgically resectable early-stage pancreatic cancer. J Natl Cancer Inst 2017;109(8): djw341.
26. Belfiori G, Crippa S, Francesca A, et al. Long-term survivors after upfront resection for pancreatic ductal adenocarcinoma: an actual 5-year analysis of disease-specific and post-recurrence survival. Ann Surg Oncol 2021;28:8249–8260.
27. Lennon AM, Buchanan AH, Kinde I, et al. Feasibility of blood testing combined with PET-CT to screen for cancer and guide intervention. Science 2020;369(6499): eabb9601.
28. Brentnall TA. Pancreatic cancer surveillance: learning as we go. Am J Gastroenterol 2011;106:955–956.
29. Jung G, Hernandez-Illan E, Moreira L, et al. Epigenetics of colorectal cancer: biomarker and therapeutic potential. Nat Rev Gastroenterol Hepatol 2020;17:111–130.
30. Debernardi S, O'Brien H, Algahmdi AS, et al. A combination of urinary biomarker panel and PancRISK score for earlier detection of pancreatic cancer: a case-control study. PLoS Med 2020;17(12):e1003489.
31. Yu MC, Ding GY, Ma P, et al. CircRNA UBAP2 serves as a sponge of miR-1294 to increase tumorigenesis in hepatocellular carcinoma through regulating c-Myc expression. Carcinogenesis 2021;42:1293–1303.

32. Wang J, Li T, Wang B. Circ-UBAP2 functions as sponges of miR-1205 and miR-382 to promote glioma progression by modulating STC1 expression. Cancer Med 2021; 10:1815–1828.
33. Liu T, Zhou L, He Z, et al. Circular RNA hsa_circ_0006117 facilitates pancreatic cancer progression by regulating the miR-96-5p/KRAS/MAPK signaling pathway. J Oncol 2021; 2021:9213205.
34. Rong Z, Shi S, Tan Z, et al. Circular RNA CircEYA3 induces energy production to promote pancreatic ductal adenocarcinoma progression through the miR-1294/c-Myc axis. Mol Cancer 2021;20:106.
35. Zhu J, Zhou Y, Zhu S, et al. circRNA circ_102049 implicates in pancreatic ductal adenocarcinoma progression through activating CD80 by targeting miR-455-3p. Mediators Inflamm 2021;2021: 8819990.

Received January 9, 2023. Accepted September 25, 2023.

Correspondence
Address correspondence to: Ajay Goel, PhD, Department of Molecular Diagnostics and Experimental Therapeutics, Beckman Research Institute of City of Hope, Biomedical Research Center, 1218 S. Fifth Avenue, Suite 2226, Monrovia, California 91016. e-mail: ajgoel@coh.org; or Guixin Zhang, MD, Department of General Surgery, The First Affiliated Hospital of Dalian Medical University, 222 Zhongshan Road, Dalian, China. e-mail: zhangguixin@dmu.edu.cn.

Acknowledgments
The authors thank Drs Milad Moloudizargari, Souvick Roy, Kota Nakamura, Silei Sui, Katsuki Miyazaki, Zhongxu Zhu, Nouni Mouallem, Keisuke Okuno, Yoh Asahi, and Yu Chen for their thoughtful discussions and advice during the course of this project.

CrediT Authorship Contributions
Caiming Xu, MD, PhD (Data curation: Lead; Formal analysis: Lead; Methodology: Lead; Writing – original draft: Lead)
Eunsung Jun, PhD (Resources: Supporting)
Yoshinaga Okugawa, MD, PhD (Conceptualization: Supporting; Resources: Supporting)
Yuji Toiyama, MD, PhD (Conceptualization: Supporting; Resources: Supporting)
Erkut Borazanci, MD (Conceptualization: Supporting; Resources: Equal)
John Bolton, MD (Conceptualization: Supporting; Resources: Equal)
Akinobu Taketomi, MD, PhD (Resources: Equal)
Song Cheol Kim, MD, PhD (Resources: Equal)
Dong Shang, MD (Resources: Supporting; Supervision: Supporting)
Daniel Von Hoff, MD (Conceptualization: Equal; Supervision: Equal)
Guixin Zhang, MD (Resources: Equal; Supervision: Equal)
Ajay Goel, PhD (Conceptualization: Lead; Funding acquisition: Lead; Writing – review & editing: Equal)

Conflicts of interest
The authors disclose no conflicts.

Funding
This work was supported by grants CA72851, CA181572, CA187956, and CA214254 from the National Cancer Institute National Institute of Health. This work was also supported by a grant from the National Natural Science Foundation of China (no. 82104594).

Data Availability
All data derived from the public database are available from the GEO database.

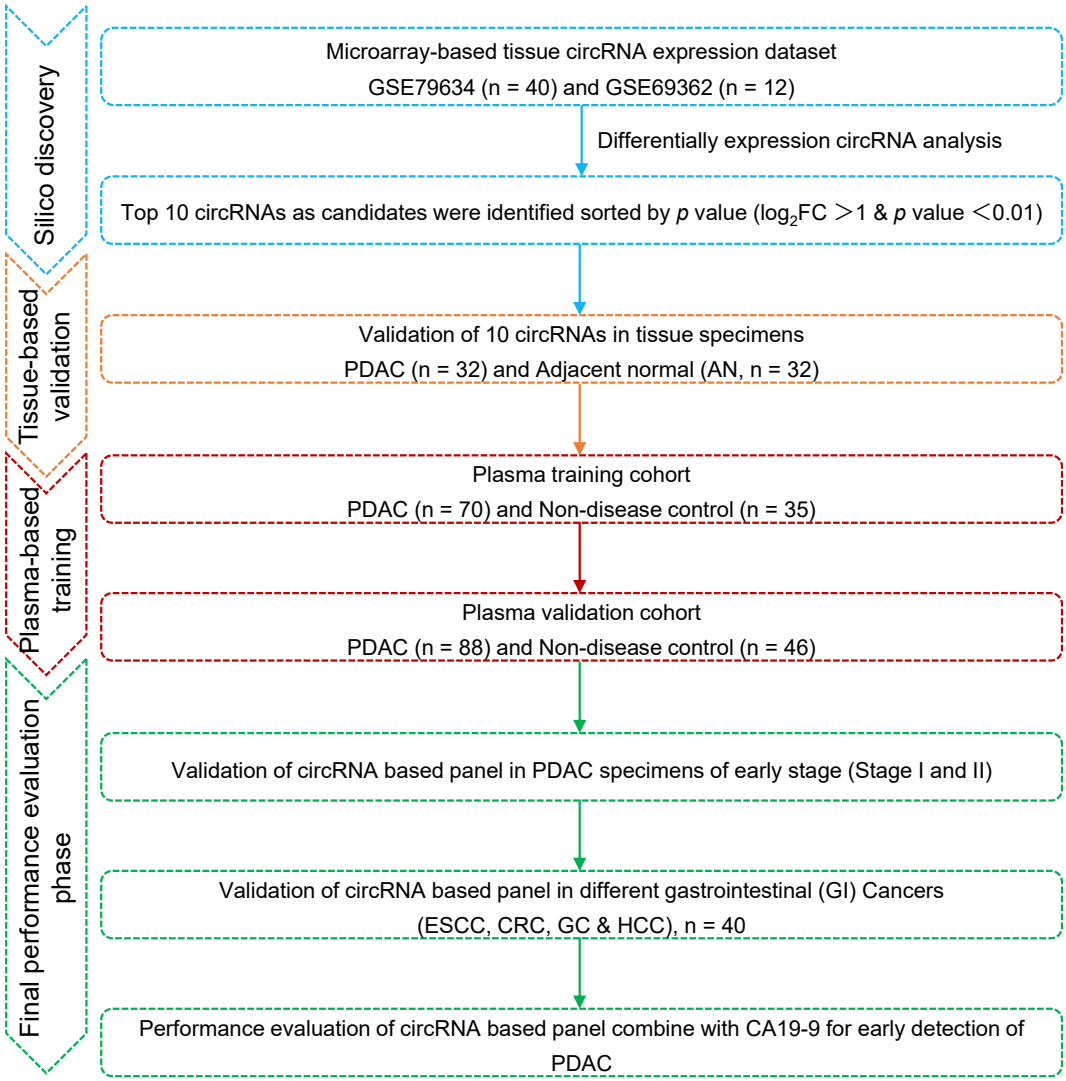

Supplementary Figure 1. Flowchart of the study design for developing a liquid biopsy–based circRNA panel of biomarkers for the early detection of PDAC.

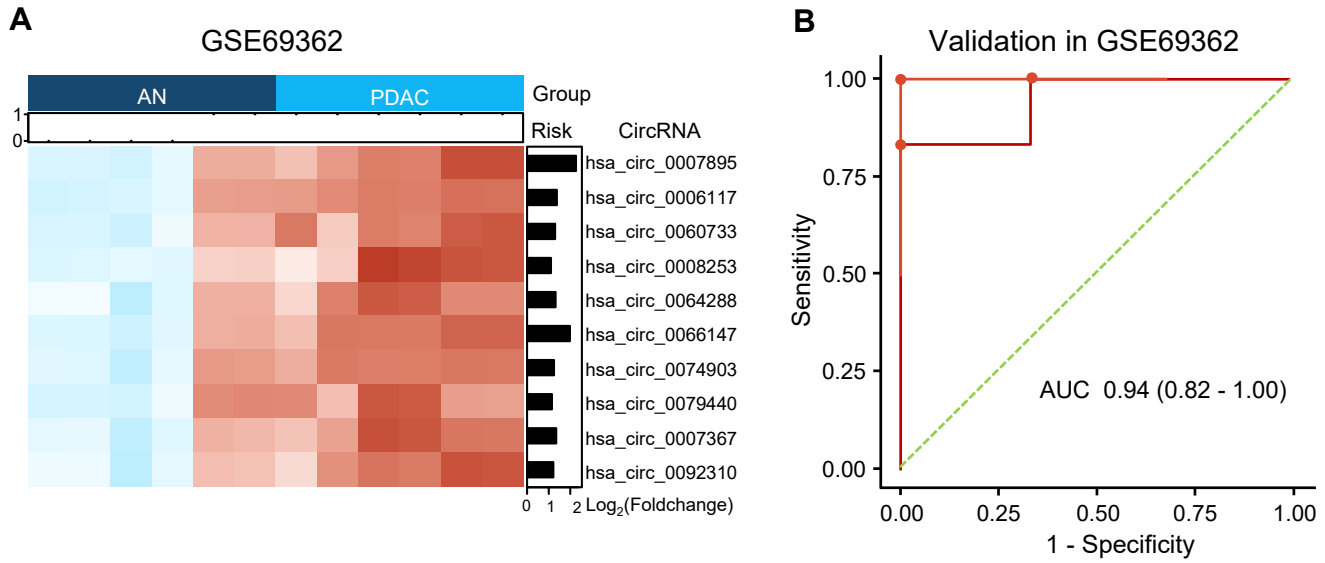

Supplementary Figure 2. Validation of the circRNA candidates for PDAC diagnosis in a genome-wide cohort, in silico. (*A*) *Heatmap* of top 10 overlapping up-regulated circRNAs (sorted by *P* value) between the tissues from patients with PDAC (n = 6) and matched AN tissues (n = 6) in the validation data set. (*B*) Performance assessment of the 10-circRNA panel ROC curve analysis. The *red lines* indicate the specificity and sensitivity with 95% CI for each circRNA under the best threshold. The *red points* show the optimal threshold for specificity and sensitivity.

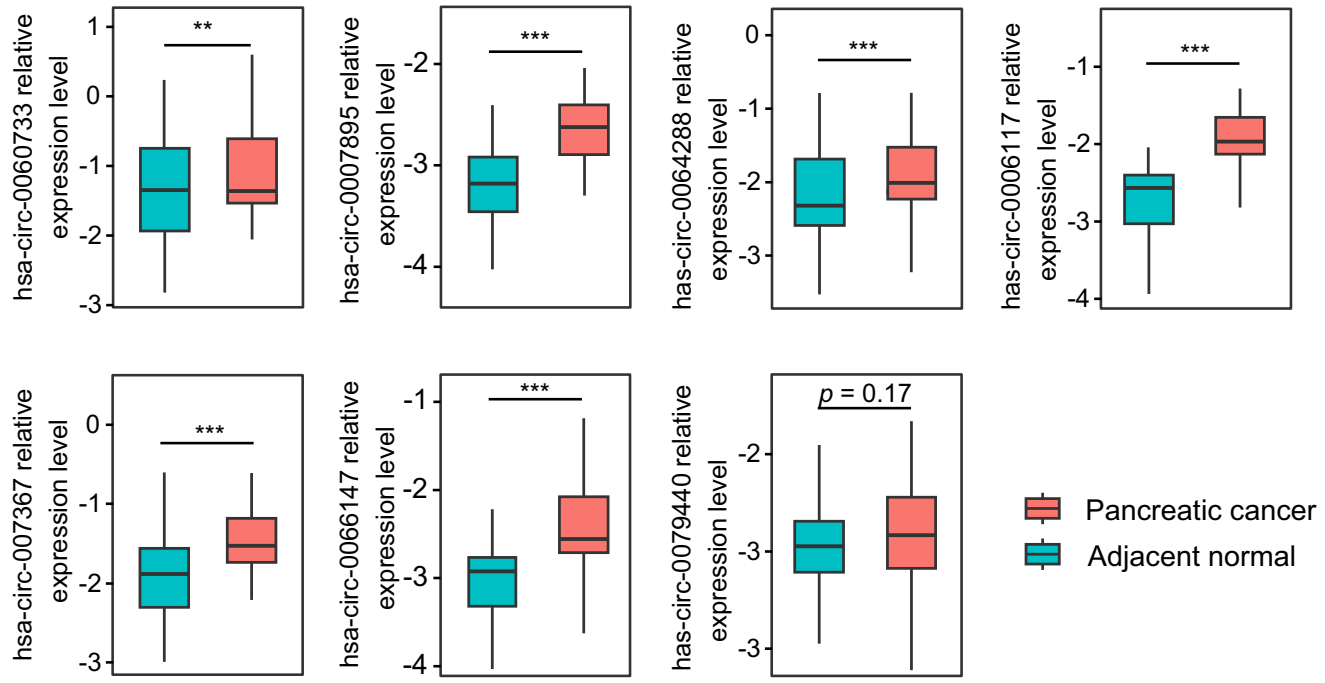

Supplementary Figure 3. Validation of the circRNA candidates for PDAC diagnosis in a genome-wide cohort, in silico. The expression level of our 7 circRNA candidates in tissue from patients with PDAC. $^{**}P < .01$; $^{***}P < .001$.

Supplementary Table 1. Clinicopathologic Characteristics of Patients With Pancreatic Ductal Adenocarcinoma From the Tissue–Based Validation Cohort

Variable	Tissue samples
Age, *y* (range)	57.5 (32–88)
Sex, n (%)	
Male	24 (75.0)
Female	8 (25.0)
TNM stage,[a] n (%)	
1 and 2	26 (81.25)
3 and 4	6 (18.75)

[a]TNM stage was based on *AJCC Cancer Staging Manual*, 8th edition.[16]

Supplementary Table 2. Clinicopathologic Characteristics of Plasma Samples From the Plasma–Based Training and Final Performance Evaluation Cohorts

	Plasma–based training			Performance evaluation cohorts			
Variable	Patients with PDAC (n = 70)	Healthy controls (n = 35)	*P* value	Patients with PDAC (n = 88)	Healthy controls (n = 46)	PCLs	*P* value
Age, *y*, mean ± SD	60.7 ± 10.6	48.5 ± 8.5[a]	<.01[a]	67.5 ± 9.2	42.4 ± 12.3[a]	63.7 ± 13.8[b]	< .01[a] .10[b]
Sex, n (%)			.09[c]				.24[d]
Male	47 (67.1)	17 (48.6)		46 (52.3)	17 (37.0)	13 (46.4)	
Female	23 (32.9)	18 (51.4)		42 (47.7)	29 (63.0)	15 (53.6)	
Race, n (%)			—				.26[d]
White	Unknown	Unknown		69 (78.4)	43 (93.5)	23 (82.1)	
Black	Unknown	Unknown		16 (18.2)	2 (4.3)	4 (14.3)	
Unknown	70 (100)	35 (100)		3 (3.4)	1 (2.2)	1 (3.6)	
TNM stage,[e] n (%)			—				—
1 and 2	48 (68.6)	NA		63 (71.6)	NA	NA	
3 and 4	22 (31.4)	NA		23 (26.1)	NA	NA	
Unknown	0 (0)	NA		2 (2.3)	NA	NA	

NA, not applicable; PCL, pancreatic cystic lesion.
[a]$P < .01$ vs patients with PDAC.
[b]$P = .1$ vs patients with PDAC, *t* test.
[c]Fisher exact test.
[d]Pearson χ^2 test.
[e]TNM stage was based on *AJCC Cancer Staging Manual*, 8th edition.[16]

Supplementary Table 3. List of the circRNA Primers Used in This Study

circRNA ID	Left primer	Right primer
hsa_circ_0007895	CTCAGGCAACCCAAACGTA	GGATTGCAAGTCTCTCTCAGC
hsa_circ_0029634	CCTACTACAGTTCCTGTTCCTGGT	CTCTTTGTTAGGTGTTGGAGAAGG
hsa_circ_0049783	ACCTCCTCAACTGGGTTCAAG	AGTGGGGGTTTCTCTGTTTCC
hsa_circ_0006117	CCAGATAACCAGTTCACGGATG	GGAATCCATGCTTATCTGAAGG
hsa_circ_0060733	TCTTTTTAAGGTTGAAGATGAACCA	ACTCGATCGGCTTCACAAAT
hsa_circ_0008253	TGGGTTCCCCTGGTGCT	CTGGTCTCTCTTCTCGGGGT
hsa_circ_0064288	GGCACTGCTCTTGAAAACCC	GGAGCACTCTGCAAATGTCAA
hsa_circ_0066147	GGTGCTTCCCTCCGGTTTTT	CTCAGGACGCAAGTCATCCA
hsa_circ_0074903	AACCACAGTGTACAGTGGACC	ATGGGCTGGTCTGCAGTAGG
hsa_circ_0079440	CCTAAACAGACAGGCTACGGA	CGTCCTCTGGTTCTCTTGGAA
hsa_circ_0007367	TACTTCTTGGGACCTCAAGCC	GTTTCAGAAAGCAAGATGACTGAG
hsa_circ_0092310	GCAGCCATATCTCCATCTGGG	AGTTCCTGGCAGGGAGTACAT
β–actin	CCTTTGCCGATCCGCCG	GATATCATCCATGGTGAGCTGG

Supplementary Table 4. The Expression Raw Data (log10[$2^{-\Delta CT}$]) of circRNAs in the Tissue–Based Validation Phase

ID	Group	hsa_circ_0060733	hsa_circ_0007895	hsa_circ_0064288	hsa_circ_0006117	hsa_circ_0007367	hsa_circ_0066147	hsa_circ_0079440
ANP1	AN	0.22451	−4.02639	−1.02699	−4.02639	−0.60959	−4.02639	−3.16479
ANP2	AN	−0.77874	−4.50302	−1.68517	−2.29879	−1.60937	−2.76095	−3.03356
ANP3	AN	0.12746	−3.20127	−0.89346	−3.94038	−0.6006	−2.73355	−2.93226
ANP4	AN	−2.2026	−2.92647	−2.72881	−2.38871	−2.2797	−3.53573	−4.26691
ANP5	AN	−0.03014	−4.33588	−1.06208	−4.59156	−0.82164	−2.3357	−1.95661
ANP6	AN	−1.08945	−3.56653	−2.61284	−3.56653	−2.60332	−3.56653	−1.46816
ANP7	AN	0.07466	−3.79008	−0.92723	−3.79008	−0.60771	−3.79008	−2.53928
ANP8	AN	0.22971	−2.65915	−0.78445	−2.73243	−0.39634	−4.18479	−2.92934
ANP9	AN	−2.82903	−3.64911	−3.53371	−2.7348	−2.99267	−3.19789	−3.42617
ANP10	AN	−1.92792	−2.75441	−2.53777	−2.03596	−2.3131	−3.50565	−2.67326
ANP11	AN	−2.03202	−3.4212	−2.73375	−2.56711	−2.47886	−3.01819	−2.75558
ANP12	AN	−2.14678	−3.02446	−2.62861	−2.16593	−2.30878	−2.85566	−4.02639
ANP13	AN	−1.37137	−3.22312	−2.39405	−2.43999	−2.04859	−3.43279	−2.68532
ANP14	AN	−1.75155	−2.95556	−2.48078	−2.40694	−2.13204	−2.84048	−2.4146
ANP15	AN	−1.77984	−2.81042	−2.34678	−2.60052	−1.89223	−2.98544	−2.94897
ANP16	AN	−1.47318	−3.15899	−2.3453	−2.67147	−1.79541	−2.75993	−1.89942
ANP17	AN	−1.40973	−4.72518	−2.09703	−3.00624	−2.00877	−2.38163	−3.51157
ANP18	AN	−0.67713	−3.40334	−1.67704	−4.80529	−1.40976	−3.27462	−3.24018
ANP19	AN	−1.2853	−3.15705	−2.2612	−3.10827	−1.8289	−2.92697	−2.90935
ANP20	AN	−0.09486	−2.89739	−1.10389	−2.45019	−0.81065	−2.44965	−3.94038
ANP21	AN	−2.3775	−2.96365	−2.76138	−2.16723	−2.30345	−3.6183	−2.72466
ANP22	AN	−2.19302	−3.87253	−2.58052	−2.84743	−2.31126	−2.97	−2.88904
ANP23	AN	−0.53243	−2.40709	−1.49722	−4.12901	−1.14688	−2.21311	−2.94542
ANP24	AN	−1.45953	−3.04249	−2.35555	−2.19426	−1.88288	−2.9082	−1.63154
ANP25	AN	−1.0441	−2.83323	−1.96827	−2.5702	−1.793	−2.3549	−3.19496
ANP26	AN	−2.06449	−3.25187	−2.81704	−2.50269	−2.37929	−3.05827	−3.12664
ANP27	AN	−1.24704	−3.0884	−2.28939	−2.28712	−1.87972	−2.84058	−3.06353
ANP28	AN	−1.12148	−3.32943	−2.00977	−2.54227	−1.70707	−2.75812	−3.79008

Supplementary Table 4. Continued

ID	Group	hsa_circ_0060733	hsa_circ_0007895	hsa_circ_0064288	hsa_circ_0006117	hsa_circ_0007367	hsa_circ_0066147	hsa_circ_0079440
ANP29	AN	−1.62377	−3.31979	−2.47249	−2.37363	−2.15901	−2.78602	−2.69603
ANP30	AN	−1.33419	−2.76682	−2.13426	−2.60258	−1.87518	−2.90583	−2.57831
ANP31	AN	−1.98493	−3.27651	−2.66211	−2.56696	−2.36735	−3.06321	−3.1108
ANP32	AN	−1.08782	−2.67223	−1.96395	−2.42322	−1.65111	−2.7501	−3.67129
PDAC1	PC	0.35449	−2.03894	−0.78033	−1.2829	−0.6076	−1.08	−2.7006
PDAC2	PC	−0.42653	−2.65123	−1.41899	−1.95681	−1.18406	−1.98177	−3.121
PDAC3	PC	0.59696	−2.59221	−0.45694	−1.66204	−0.26839	−1.18113	−3.07256
PDAC4	PC	−1.37695	−2.25182	−2.03238	−1.35523	−1.50001	−2.27024	−3.39464
PDAC5	PC	0.10203	−2.60736	−0.95118	−2.12116	−0.83948	−1.50498	−2.44541
PDAC6	PC	−0.64006	−2.4088	−1.55606	−1.60696	−1.30432	−1.93898	−3.08754
PDAC7	PC	1.2259	−3.29778	0.18417	−1.7435	0.45584	−1.68313	−3.15421
PDAC8	PC	1.02731	−3.93434	−0.10518	−2.16533	0.1794	−1.41293	−2.43633
PDAC9	PC	−1.66743	−2.23808	−2.42375	−1.32566	−1.62801	−2.57378	−3.20844
PDAC10	PC	−1.52171	−4.19911	−3.23373	−2.56943	−2.21009	−3.62163	−3.93044
PDAC11	PC	−1.58849	−2.81796	−2.22423	−1.97831	−1.79916	−2.57947	−2.51311
PDAC12	PC	−0.89322	−2.95017	−1.78745	−2.28434	−1.58827	−2.20053	−2.94863
PDAC13	PC	−1.43565	−2.96858	−2.08257	−2.06325	−1.47409	−2.69872	−2.12613
PDAC14	PC	−1.32429	−2.41552	−1.90315	−1.69745	−1.53891	−2.32568	−2.96886
PDAC15	PC	−1.28223	−2.35636	−2.1372	−2.06709	−1.70204	−2.42598	−2.14168
PDAC16	PC	−0.84758	−2.38558	−1.64239	−1.70044	−1.16772	−2.5792	−1.65484
PDAC17	PC	−1.42367	−2.8938	−2.20637	−2.32534	−1.95021	−2.59885	−3.00744
PDAC18	PC	−0.69692	−2.63705	−1.73398	−1.87296	−1.3555	−2.51202	−4.21325
PDAC19	PC	−2.05964	−2.89401	−2.59974	−2.10241	−2.17925	−3.26016	−3.33779
PDAC20	PC	−0.16133	−2.43318	−1.3373	−2.16848	−0.99187	−2.08645	−2.95091
PDAC21	PC	−1.62014	−2.53896	−2.2139	−2.07252	−1.85664	−2.55282	−2.59532
PDAC22	PC	−1.73897	−2.47345	−2.24348	−1.48841	−1.73195	−2.70577	−2.62865
PDAC23	PC	−0.97768	−2.67047	−1.8537	−1.73872	−1.56233	−2.62651	−2.39868
PDAC24	PC	−1.59438	−2.3871	−2.09773	−1.63849	−1.48491	−2.88574	−2.03352

Supplementary Table 4. Continued

ID	Group	hsa_circ_0060733	hsa_circ_0007895	hsa_circ_0064288	hsa_circ_0006117	hsa_circ_0007367	hsa_circ_0066147	hsa_circ_0079440
PDAC25	PC	–1.71942	–3.14199	–2.31848	–2.82217	–2.17018	–3.05608	–3.20358
PDAC26	PC	–1.44686	–3.00751	–2.28621	–2.25216	–1.90276	–2.72662	–2.55441
PDAC27	PC	–1.37515	–2.72104	–2.13814	–1.83705	–1.74675	–2.54808	–3.27109
PDAC28	PC	–1.34856	–2.30207	–1.86219	–1.5702	–1.58826	–2.05058	–4.18479
PDAC29	PC	–1.66608	–2.53319	–2.37927	–2.04587	–1.71491	–2.70674	–2.15892
PDAC30	PC	–1.46683	–2.66656	–1.98368	–2.04209	–1.45979	–2.92686	–2.43668
PDAC31	PC	–1.47994	–2.70996	–2.57443	–2.54328	–1.51162	–3.05449	–2.08981
PDAC32	PC	–0.52985	–2.34766	–1.38271	–1.54073	–0.95935	–2.07893	–2.43522

Supplementary Table 5. Summary of the Diagnostic Performance of Individual circRNAs in the Issue-Based Validation Cohort

circRNA ID	AUC (95% CI)	Accuracy (95% CI)	PPV (95% CI)	Sensitivity (95% CI)	Specificity (95% CI)	NPV (95% CI)
hsa_circ_0060733	0.59 (0.44–0.83)	0.52 (0.42–0.61)	0.51 (0.45–0.57)	0.84 (0.72–0.97)	0.19 (0.06–0.34)	0.55 (0.25–0.83)
hsa_circ_0007895	0.84 (0.74–0.94)	0.80 (0.70–0.89)	0.88 (0.76–1.00)	0.69 (0.53–0.85)	0.91 (0.78–1.00)	0.74 (0.65–0.85)
hsa_circ_0064288	0.65 (0.51–0.79)	0.67 (0.56–0.77)	0.63 (0.54–0.72)	0.84 (0.72–0.97)	0.50 (0.31–0.66)	0.76 (0.61–0.93)
hsa_circ_0006117	0.92 (0.86–0.99)	0.88 (0.78– 0.95)	0.88 (0.78–0.97)	0.88 (0.75–0.97)	0.88 (0.75–0.97)	0.88 (0.78–0.97)
hsa_circ_0007367	0.71 (0.57–0.84)	0.72 (0.61–0.83)	0.69 (0.59–0.81)	0.78 (0.62–0.91)	0.66 (0.50–0.81)	0.75 (0.62–0.89)
hsa_circ_0066147	0.82 (0.71–0.92)	0.83 (0.73–0.91)	0.84 (0.73–0.96)	0.81 (0.66–0.94)	0.84 (0.72–0.97)	0.82 (0.71–0.93)
hsa_circ_0079440	0.56 (0.42–0.71)	0.62 (0.52–0.73)	0.68 (0.52–0.84)	0.47 (0.31–0.66)	0.78 (0.62–0.91)	0.60 (0.51–0.69)

Supplementary Table 6. The Expression Raw Data (log10[$2^{-\Delta CT}$]) of circRNAs in the Plasma–Based Training Phase

ID	Group	hsa_circ_0060733	hsa_circ_0006117	hsa_circ_0064288	hsa_circ_0007895	hsa_circ_0007367
Nondisease control1	Healthy control	–2.70809	–1.92978	–2.51925	–6.98083	–1.19645
Nondisease control2	Healthy control	–3.29755	–3.29755	–4.8027	–3.80278	–3.29755
Nondisease control3	Healthy control	–3.56807	–1.74679	–5.07322	–6.57837	–1.81134
Nondisease control4	Healthy control	–3.40969	–2.08664	–3.49886	–7.56063	–2.66895
Nondisease control5	Healthy control	–3.86147	–1.49485	–5.36662	–6.87177	–1.90134
Nondisease control6	Healthy control	–2.55477	–2.52166	–2.46234	–7.04168	–2.88451
Nondisease control7	Healthy control	–2.71311	–1.71819	–2.58866	–7.23214	–1.94052
Nondisease control8	Healthy control	–3.01518	–3.01518	–4.52033	–2.68956	–2.30342
Nondisease control9	Healthy control	–3.32364	–1.55429	–4.82879	–5.51742	–3.90886
Nondisease control10	Healthy control	–2.98579	–1.59921	–1.75658	–6.78814	–2.19538
Nondisease control11	Healthy control	–3.42147	–2.24006	–4.92662	–6.43177	–1.79864
Nondisease control12	Healthy control	–3.391	–1.86882	–4.76213	–6.4013	–1.52532
Nondisease control13	Healthy control	–2.89845	–1.40031	–4.10193	–2.68643	–1.72569
Nondisease control14	Healthy control	–1.70612	–2.12555	–1.12147	–6.32737	–1.18934
Nondisease control15	Healthy control	–2.63821	–2.31021	–5.28908	–6.79423	–2.07434
Nondisease control16	Healthy control	–2.48911	–1.72901	–5.46822	–2.67252	–1.60385
Nondisease control17	Healthy control	–3.26546	–2.02817	–4.77061	–6.27576	–2.73535
Nondisease control18	Healthy control	–3.17318	–1.94619	–3.17995	–2.95546	–2.29171
Nondisease control19	Healthy control	–2.2282	–3.75698	–3.75714	–6.76728	–0.22467
Nondisease control20	Healthy control	–2.47747	–1.7149	–2.84652	–6.94146	–1.77116
Nondisease control21	Healthy control	–1.96889	–1.2439	–4.51214	–6.01729	–1.8688
Nondisease control22	Healthy control	–2.13949	–3.29933	–4.80448	–1.74442	–1.61337
Nondisease control23	Healthy control	–3.76242	–2.76849	–5.49133	–6.99648	–4.61355
Nondisease control24	Healthy control	–3.636	–2.67281	–5.7147	–7.21985	–2.61771
Nondisease control25	Healthy control	–2.6832	–2.20182	–2.03071	–6.64475	–1.04174
Nondisease control26	Healthy control	–2.8529	–1.73064	–3.04817	–2.49366	–1.88053
Nondisease control27	Healthy control	–3.15562	–1.18629	–4.2983	–6.16592	–1.19496
Nondisease control28	Healthy control	–3.38665	–1.48723	–5.40374	–6.90889	–1.44291
Nondisease control29	Healthy control	–2.26421	–2.32028	–4.90957	–6.41472	–2.42802
Nondisease control30	Healthy control	–2.83301	–1.92632	–2.96006	–7.12816	–2.13728
Nondisease control31	Healthy control	–2.16239	–2.2089	–2.02522	–2.04499	–1.21754
Nondisease control32	Healthy control	–2.07303	–1.93875	–2.1773	–2.25395	–1.76221
Nondisease control33	Healthy control	–3.48851	–1.90847	–4.99366	–6.49881	–3.95588
Nondisease control34	Healthy control	–2.97258	–2.30134	–2.807	–2.53623	–1.92183
Nondisease control35	Healthy control	–3.91681	–1.82496	–5.42196	–6.92711	–1.56321
PDAC1	PDAC	–2.14439	–2.07874	–3.72319	–2.57672	–3.04171
PDAC2	PDAC	–2.39564	–1.94872	–4.15085	–6.71002	–1.42329
PDAC3	PDAC	–2.54747	–1.61229	–2.37471	–2.30949	–1.71958
PDAC4	PDAC	–2.36424	–1.44651	–1.91629	–6.65334	–1.4413

Supplementary Table 6. Continued

ID	Group	hsa_circ_0060733	hsa_circ_0006117	hsa_circ_0064288	hsa_circ_0007895	hsa_circ_0007367
PDAC5	PDAC	–2.62116	–2.00893	–3.43751	–3.65977	–1.85093
PDAC6	PDAC	–2.7042	–1.95899	–2.44693	–2.52334	–2.16908
PDAC7	PDAC	–1.23537	–1.67875	–4.46952	–4.13428	–0.54351
PDAC8	PDAC	–2.94131	–1.57427	–5.66606	–2.65236	–1.70284
PDAC9	PDAC	–2.46369	–1.34397	–5.32278	–5.42608	–1.89067
PDAC10	PDAC	–2.7647	–2.00109	–3.28117	–3.27041	–0.78114
PDAC11	PDAC	–3.04336	–2.03886	–5.66756	–2.93687	–2.09398
PDAC12	PDAC	–2.41585	–1.72977	–4.44779	–6.95045	–1.89031
PDAC13	PDAC	–2.89953	–2.13919	–5.34644	–4.93722	–2.06957
PDAC14	PDAC	–2.93007	–1.48303	–2.13412	–6.42446	–1.78273
PDAC15	PDAC	–1.27931	–2.8299	–2.40297	–1.53911	–0.57994
PDAC16	PDAC	–3.05343	–1.71462	–5.93703	–2.48543	–1.57148
PDAC17	PDAC	–2.06521	–1.49822	–2.342	–2.13932	–0.54932
PDAC18	PDAC	–2.63049	–1.63474	–3.0248	–3.13858	–1.7
PDAC19	PDAC	–2.03277	–1.83062	–2.31175	–6.14549	–1.77865
PDAC20	PDAC	–2.43261	–2.20783	–2.64423	–1.75133	–2.94077
PDAC21	PDAC	–2.28052	–1.63439	–2.22722	–2.69359	–1.99669
PDAC22	PDAC	–1.63623	–1.80449	–4.9472	–1.81813	–1.86645
PDAC23	PDAC	–2.44688	–1.69189	–1.76285	–7.21674	–1.53776
PDAC24	PDAC	–2.7099	–1.78981	–2.744	–2.55878	–2.47766
PDAC25	PDAC	–1.14817	–1.57715	–1.69177	–1.29313	–0.65971
PDAC26	PDAC	–2.74393	–1.23778	–2.04456	–2.90639	–1.68799
PDAC27	PDAC	–3.04117	–1.87441	–5.51287	–3.1632	–1.63707
PDAC28	PDAC	–3.01472	–1.89107	–5.68394	–7.18909	–1.70344
PDAC29	PDAC	–1.90599	–3.25578	–3.20182	–2.0034	–1.26752
PDAC30	PDAC	–2.34139	–1.91408	–3.01867	–6.16049	–2.00884
PDAC31	PDAC	–1.51531	–1.31265	–2.65533	–3.88335	–0.76897
PDAC32	PDAC	–2.00166	–1.70692	–5.65617	–2.43098	–2.17741
PDAC33	PDAC	–2.1491	–2.21689	–5.46318	–6.96833	–2.02117
PDAC34	PDAC	–2.52385	–1.82125	–2.91765	–2.14674	–1.206
PDAC35	PDAC	–1.93984	–1.41371	–1.69045	–6.30875	–1.17367
PDAC36	PDAC	–3.10199	–1.83154	–3.49788	–7.2315	–1.93002
PDAC37	PDAC	–1.74582	–1.91507	–3.62191	–2.31366	–1.55418
PDAC38	PDAC	–2.95131	–1.84051	–2.25883	–2.87063	–1.89388
PDAC39	PDAC	–0.47505	–1.49242	–1.79705	–2.10099	–1.17145
PDAC40	PDAC	–2.1382	–1.75629	–2.2563	–6.73524	–1.85665
PDAC41	PDAC	–1.65278	–1.72171	–2.54596	–2.08351	–1.21531
PDAC42	PDAC	–1.38645	–1.633	–4.8423	–1.75437	–1.5341

Supplementary Table 6. Continued

ID	Group	hsa_circ_0060733	hsa_circ_0006117	hsa_circ_0064288	hsa_circ_0007895	hsa_circ_0007367
PDAC43	PDAC	–2.35284	–2.02153	–5.64659	–2.24473	–1.54127
PDAC44	PDAC	–1.14257	–2.78194	–3.54609	–1.25301	0.02741
PDAC45	PDAC	–2.38793	–1.51668	–3.49238	–2.888	–1.97861
PDAC46	PDAC	–2.10262	–1.71036	–3.45951	–6.94111	–1.66564
PDAC47	PDAC	–2.87705	–1.81965	–2.27477	–6.87007	–1.91161
PDAC48	PDAC	–2.45428	–2.08717	–3.06492	–2.66948	–2.40879
PDAC49	PDAC	–0.03	–2.71964	–1.40677	–5.72994	–1.1782
PDAC50	PDAC	–2.70508	–2.11619	–2.14829	–2.78092	–1.46098
PDAC51	PDAC	–2.03824	–2.00943	–1.77312	–6.53443	–1.0703
PDAC52	PDAC	–2.62954	–1.5782	–1.88322	–2.60357	–1.67657
PDAC53	PDAC	–1.50822	–3.12939	–4.63454	–1.61639	–0.44537
PDAC54	PDAC	–2.32317	–1.51052	–3.89661	–2.60199	–1.64447
PDAC55	PDAC	–2.92342	–1.77332	–4.79098	–7.37741	–1.76819
PDAC56	PDAC	–3.70713	–2.16514	–2.92998	–3.97835	–1.9896
PDAC57	PDAC	–2.75521	–2.02052	–3.89573	–7.43369	–2.16522
PDAC58	PDAC	–2.44421	–1.79255	–2.63102	–7.01335	–1.26559
PDAC59	PDAC	–2.33818	–1.48112	–5.23466	–4.85784	–2.19362
PDAC60	PDAC	–2.08719	–2.18072	–4.92084	–1.87164	–3.41569
PDAC61	PDAC	–2.17156	–1.49015	–1.88834	–2.07831	–1.04543
PDAC62	PDAC	–2.43907	–1.42832	–1.69186	–6.5532	–1.98551
PDAC63	PDAC	–3.28957	–1.56156	–2.60449	–2.51909	–1.8081
PDAC64	PDAC	–1.88999	–1.98119	–1.19567	–6.34821	–1.29664
PDAC65	PDAC	–2.64353	–1.51069	–2.82574	–2.33583	–1.08692
PDAC66	PDAC	–2.75459	–1.79206	–4.92193	–7.63708	–2.76182
PDAC67	PDAC	–2.01568	–1.55828	–5.24759	–2.41599	–1.01366
PDAC68	PDAC	–2.59062	–1.56292	–2.80505	–2.87316	–1.68784
PDAC69	PDAC	–2.62346	–1.56174	–2.24989	–2.75632	–1.68813
PDAC70	PDAC	–2.31923	–1.19354	–5.37153	–2.82273	–1.34047

Supplementary Table 7. Univariate Analysis for the circRNA Candidates in the Plasma-Based Training Cohort

circRNA ID	Odds ratio (95% CI)	Estimate	*P* value
hsa_circ_0060733	3.77 (3.13–4.41)	1.33	<.001
hsa_circ_0006117	1.70 (1.28–2.13)	0.53	.015
hsa_circ_0064288	1.52 (1.10–1.94)	0.42	.051
hsa_circ_0007895	2.18 (1.73–2.63)	0.78	<.001
hsa_circ_0007367	1.88 (1.42–2.35)	0.63	.008

Supplementary Table 8. Summary of the Diagnostic Performance of the Individual circRNAs in the Plasma–Based Training Cohort

circRNA ID	AUC (95% CI)	Accuracy (95% CI)	PPV (95% CI)	Sensitivity (95% CI)	Specificity (95% CI)	NPV (95% CI)
hsa_circ_0060733	0.77 (0.67–0.87)	0.77 (0.70–0.85)	0.79 (0.73–0.85)	0.90 (0.83–0.96)	0.51 (0.34–0.69)	0.72 (0.57–0.88)
hsa_circ_0006117	0.65 (0.53–0.76)	0.72 (0.65–0.79)	0.74 (0.69–0.79)	0.90 (0.83–0.96)	0.37 (0.20–0.54)	0.65 (0.45–0.83)
hsa_circ_0064288	0.61 (0.50–0.73)	0.65 (0.56–0.74)	0.76 (0.69–0.84)	0.69 (0.59–0.79)	0.57 (0.40–0.74)	0.48 (0.37–0.60)
hsa_circ_0007895	0.69 (0.58–0.80)	0.70 (0.61–0.78)	0.83 (0.75–0.91)	0.69 (0.57–0.79)	0.71 (0.57–0.86)	0.53 (0.44–0.64)
hsa_circ_0007367	0.64 (0.53–0.76)	0.72 (0.66–0.79)	0.74 (0.69–0.79)	0.91 (0.84–0.97)	0.34 (0.20–0.49)	0.67 (0.47–0.89)

Supplementary Table 9. The Expression Raw Data (log10[$2^{-\Delta CT}$]) of circRNAs in the Final Performance Evaluation Phase

ID	Group	hsa_circ_0060733	hsa_circ_0006117	hsa_circ_0064288	hsa_circ_0007895	hsa_circ_0007367
Nondisease control1	Healthy control	–2.74784	–1.5948	–2.62156	–6.00288	–1.28947
Nondisease control2	Healthy control	–3.07573	–1.25603	–4.58088	–1.76977	–1.07529
Nondisease control3	Healthy control	–1.79742	–1.16506	–4.35271	–5.43245	–1.74848
Nondisease control4	Healthy control	–2.87426	–2.87426	–4.37941	–5.88456	1.64022
Nondisease control5	Healthy control	–2.44684	–1.35831	–3.95199	–5.45714	–1.27197
Nondisease control6	Healthy control	–2.26265	–1.66141	–3.01418	–6.51175	–3.31868
Nondisease control7	Healthy control	–1.5636	–1.59352	–2.50655	–3.71065	–1.2688
Nondisease control8	Healthy control	–2.51835	–2.51835	–4.0235	–4.66051	–0.98534
Nondisease control9	Healthy control	–1.68451	–2.72667	–4.23182	–5.25013	–0.31333
Nondisease control10	Healthy control	–1.49071	–0.68069	–4.05875	–5.5639	–1.04054
Nondisease control11	Healthy control	–2.75724	–1.54568	–4.43916	–5.94431	–1.38119
Nondisease control12	Healthy control	–2.73344	–1.77145	–5.01305	–2.90871	–2.0384
Nondisease control13	Healthy control	–2.12254	–2.10002	–5.19704	–6.70219	–2.28093
Nondisease control14	Healthy control	–2.61875	–1.46651	–2.98541	–3.98436	–1.44208
Nondisease control15	Healthy control	–2.96291	–2.96291	–4.46806	–4.42829	–1.71452
Nondisease control16	Healthy control	–3.22087	–1.85973	–4.72602	–6.23117	–3.22087
Nondisease control17	Healthy control	–2.92792	–1.59266	–4.43307	–1.71798	–1.77441
Nondisease control18	Healthy control	–2.18602	–2.00822	–4.66311	–6.16826	–1.70148
Nondisease control19	Healthy control	–2.32474	–1.74857	–5.03917	–2.32511	–1.52042
Nondisease control20	Healthy control	–2.12685	–1.82528	–4.96317	–6.46832	–3.45802
Nondisease control21	Healthy control	–3.02462	–3.02462	–3.74083	–6.03492	–1.64645
Nondisease control22	Healthy control	–1.53736	–1.27088	–4.13373	–5.63888	–2.62858
Nondisease control23	Healthy control	–3.07262	–3.07262	–4.57777	–6.08292	–1.54928
Nondisease control24	Healthy control	–2.6116	–1.6795	–5.08692	–2.32754	–1.92202
Nondisease control25	Healthy control	–1.65134	–1.04715	–4.35797	–5.86312	–1.52234
Nondisease control26	Healthy control	–1.81446	–1.97159	–3.12325	–6.32261	–2.4455
Nondisease control27	Healthy control	–2.0119	–1.14483	–2.67218	–1.53793	–1.99159
Nondisease control28	Healthy control	–1.7345	–1.43583	–2.64572	–5.80851	–2.79821
Nondisease control29	Healthy control	–2.99673	–2.99673	–4.50188	–6.00703	–1.76711
Nondisease control30	Healthy control	–2.47064	–1.48742	–3.45594	–5.90101	–1.81343
Nondisease control31	Healthy control	–2.58293	–1.35914	–3.2079	–5.59323	–1.7504
Nondisease control32	Healthy control	–1.96444	–2.19689	–2.89789	–6.0954	–3.0851
Nondisease control33	Healthy control	–2.84557	0.41608	–4.35072	–5.85587	0.35209
Nondisease control34	Healthy control	–1.67884	–1.60759	–3.26302	–5.86702	–0.04628
Nondisease control35	Healthy control	–2.971	–1.89838	–4.60057	–3.10466	–2.24472
Nondisease control36	Healthy control	–3.77743	–1.64908	–5.28258	–5.28619	–1.64704
Nondisease control37	Healthy control	–3.11606	–1.71788	–4.62121	–6.12636	–1.45651
Nondisease control38	Healthy control	–1.49145	–2.53428	–2.45094	–5.54458	–2.53428
Nondisease control39	Healthy control	–2.95093	–1.63339	–4.45608	–5.96123	–2.95093

Supplementary Table 9. Continued

ID	Group	hsa_circ_0060733	hsa_circ_0006117	hsa_circ_0064288	hsa_circ_0007895	hsa_circ_0007367
Nondisease control40	Healthy control	–2.22987	–1.74732	–4.55724	–6.06239	–3.05209
Nondisease control41	Healthy control	–4.72	–2.79698	–6.22515	–3.37678	–2.40026
Nondisease control42	Healthy control	–3.05155	–1.90912	–4.5567	–3.79081	–1.6679
Nondisease control43	Healthy control	–2.79804	–1.47232	–4.30319	–5.80834	–2.79804
Nondisease control44	Healthy control	–2.99713	–1.61792	–4.50228	–6.00743	–1.30377
Nondisease control45	Healthy control	–2.69178	–1.29936	–2.20034	–5.70208	0.62764
Nondisease control46	Healthy control	–3.06068	–1.88139	–5.63776	–2.38854	–2.08002
PDAC1	PDAC	–1.32302	–1.53663	–2.13986	–1.54777	–1.33518
PDAC2	PDAC	–2.13557	–0.9142	–2.35823	–6.41097	–0.99559
PDAC3	PDAC	–2.04768	–0.89202	–2.61007	–4.64974	–1.24841
PDAC4	PDAC	–1.84496	–1.28334	–4.1554	–1.83421	–1.51966
PDAC5	PDAC	–2.51994	–1.04289	–4.52845	–1.57851	–1.47781
PDAC6	PDAC	–2.34702	–2.34702	–3.85217	–1.0179	–1.01157
PDAC7	PDAC	–2.02623	–0.84184	–4.49545	–1.95937	–0.77414
PDAC8	PDAC	–2.89533	–1.0798	–1.89913	–4.24422	–0.86284
PDAC9	PDAC	–1.87394	–1.57322	–2.37837	–4.07306	–0.82311
PDAC10	PDAC	–1.87998	–2.69522	–2.49836	–1.42237	–2.69522
PDAC11	PDAC	–0.96027	–1.32781	–1.50082	–1.41358	–0.89024
PDAC12	PDAC	–1.52705	–2.30468	–3.80983	–4.59046	–1.00611
PDAC13	PDAC	–1.65635	–1.385	–4.23575	–5.59876	–2.65987
PDAC14	PDAC	–1.64952	–1.60653	–2.71372	–5.98185	–1.58317
PDAC15	PDAC	–1.86744	–3.26432	–2.28808	–2.45234	–1.6669
PDAC16	PDAC	–1.73321	–1.33468	–2.31502	–4.18409	–1.18427
PDAC17	PDAC	–2.72261	–2.72261	–4.22776	–5.73291	–0.99129
PDAC18	PDAC	–2.22598	–1.04755	–4.49124	–1.52393	–1.6916
PDAC19	PDAC	–1.06062	–1.0454	–4.21788	–5.72303	–0.74008
PDAC20	PDAC	–1.39698	–1.17004	–2.2336	–2.17092	–2.03694
PDAC21	PDAC	–1.68914	–1.18312	–4.82998	–2.02035	–1.58007
PDAC22	PDAC	–1.74365	–1.45485	–4.58608	–6.09123	–1.69012
PDAC23	PDAC	–2.44479	–1.10137	–3.94994	–1.02813	–1.43779
PDAC24	PDAC	–2.07778	–0.95158	–2.96206	–6.05809	–1.62291
PDAC25	PDAC	–2.77634	–1.1552	–4.13394	–5.78664	–1.87543
PDAC26	PDAC	–1.49207	–1.58434	–2.72399	–1.34371	–1.37608
PDAC27	PDAC	–1.85849	–1.07918	–4.24944	–1.89022	–1.12559
PDAC28	PDAC	–1.09451	–1.15286	–4.0704	–1.72	–1.5647
PDAC29	PDAC	–3.01799	–1.05965	–2.9037	–1.95076	–2.44812
PDAC30	PDAC	–3.02104	–1.107	–4.52619	–6.03134	–1.20735
PDAC31	PDAC	–2.20898	–3.05703	–4.07123	–1.99537	–1.55149

Supplementary Table 9. Continued

ID	Group	hsa_circ_0060733	hsa_circ_0006117	hsa_circ_0064288	hsa_circ_0007895	hsa_circ_0007367
PDAC32	PDAC	−1.76601	−0.60969	−4.61611	−1.94542	−1.09488
PDAC33	PDAC	−1.68891	−1.09238	−4.56593	−6.07108	−1.28597
PDAC34	PDAC	−1.70245	−0.97993	−4.27051	−5.77566	−1.50573
PDAC35	PDAC	−2.94452	−1.58465	−4.44967	−5.95482	−1.06869
PDAC36	PDAC	−1.53059	−1.16491	−4.51971	−1.45757	−3.01456
PDAC37	PDAC	−2.77056	−2.77056	−3.36973	−4.94223	−1.9619
PDAC38	PDAC	−1.30657	−0.75554	−2.65732	−1.79028	−1.18185
PDAC39	PDAC	−2.76566	−1.41178	−4.27081	−1.49454	−2.20776
PDAC40	PDAC	−2.38887	−1.19953	−3.89183	−2.07221	−1.01259
PDAC41	PDAC	−2.77738	−1.07641	−2.29514	−3.73193	−1.35865
PDAC42	PDAC	−1.23661	−2.53491	−4.04006	−1.00685	−2.53491
PDAC43	PDAC	−1.22963	−1.14842	−4.02783	−5.53298	−2.52268
PDAC44	PDAC	−1.60334	−0.72086	−4.37614	−1.56546	−1.75133
PDAC45	PDAC	−1.63259	−1.29712	−2.55491	−1.74567	−1.46728
PDAC46	PDAC	−3.22049	−1.8837	−2.48999	−6.23079	−1.23205
PDAC47	PDAC	−2.03402	−0.95493	−4.57392	−6.07907	−2.25265
PDAC48	PDAC	−1.62335	−1.75254	−4.50985	−1.49187	−1.30406
PDAC49	PDAC	−2.02861	−1.46872	−2.1478	−1.60922	−1.27633
PDAC50	PDAC	−1.81903	−0.7811	−2.69458	−5.93124	−0.67024
PDAC51	PDAC	−2.53251	−0.90911	−1.96158	−1.51277	−2.53251
PDAC52	PDAC	−1.60122	−1.17228	−2.25796	−1.30729	−0.11747
PDAC53	PDAC	−2.84292	−0.95958	−4.34807	−5.85322	−1.23187
PDAC54	PDAC	−2.57547	−2.57547	−3.67103	−1.34024	−1.6273
PDAC55	PDAC	−1.46158	−1.39552	−4.53475	−6.0399	−1.13282
PDAC56	PDAC	−1.04259	−1.46257	−1.46011	−5.80103	−1.41222
PDAC57	PDAC	−1.35896	−2.64749	−1.78235	−5.65779	−1.018
PDAC58	PDAC	−1.80478	−1.01075	−2.38118	−1.56579	−1.47799
PDAC59	PDAC	−2.60267	−0.29913	−3.04702	−1.04869	−0.97931
PDAC60	PDAC	−1.10588	−2.52897	−1.57027	−0.19685	−0.89483
PDAC61	PDAC	−2.49617	−1.13661	−4.48404	−1.67438	−1.73855
PDAC62	PDAC	−2.3869	−1.18834	−2.34966	−1.96505	−0.63388
PDAC63	PDAC	−1.72158	−2.73641	−4.24156	−4.66061	−0.76638
PDAC64	PDAC	−3.13221	−1.06335	−1.43632	−1.76814	−1.40485
PDAC65	PDAC	−1.68673	−2.04381	−3.63133	−6.44036	−2.59311
PDAC66	PDAC	−2.57012	−0.92049	−3.13511	−1.84826	−1.96408
PDAC67	PDAC	−1.19299	−1.55934	−2.03011	−1.74136	−0.95118
PDAC68	PDAC	−0.97748	−0.60776	−1.55959	−5.51189	−0.30411
PDAC69	PDAC	−1.38708	−2.74527	−4.25042	−1.52431	−1.11512

Supplementary Table 9. Continued

ID	Group	hsa_circ_0060733	hsa_circ_0006117	hsa_circ_0064288	hsa_circ_0007895	hsa_circ_0007367
PDAC70	PDAC	–1.85937	–1.31002	–4.45587	–2.04326	–1.3787
PDAC71	PDAC	–2.3931	–1.25365	–4.52762	–0.93003	–0.75837
PDAC72	PDAC	–2.7392	–1.04418	–5.31626	–2.63093	–1.4517
PDAC73	PDAC	–2.33734	–0.87152	–2.18079	–2.45625	–0.16566
PDAC74	PDAC	–1.84056	–1.42926	–2.53588	–6.07463	–3.06433
PDAC75	PDAC	–1.34222	–1.12083	–1.16999	–1.13869	–2.44522
PDAC76	PDAC	–2.78315	–0.86298	–2.39896	–5.79345	–2.78315
PDAC77	PDAC	–2.73772	–1.23173	–3.36105	–2.4168	–1.77962
PDAC78	PDAC	–1.863	–1.64243	–4.38396	–5.88911	–1.29813
PDAC79	PDAC	–0.85831	–2.79226	–1.85363	–5.80256	0.53999
PDAC80	PDAC	–2.00318	–2.03626	–2.31885	–1.7909	–1.34874
PDAC81	PDAC	–1.42929	–0.86592	–3.04318	–3.28295	–1.04805
PDAC82	PDAC	–2.77517	–1.12763	–1.8262	–0.63159	0.2876
PDAC83	PDAC	–1.74949	–0.69117	–4.31774	–1.2145	–2.81259
PDAC84	PDAC	–0.87056	–3.00066	–2.19132	–1.77608	–0.95998
PDAC85	PDAC	–0.7683	–0.29262	–3.84746	–5.35261	–0.86042
PDAC86	PDAC	–3.05145	–0.98064	–4.5566	–2.79943	–1.36945
PDAC87	PDAC	–1.99227	–3.00683	–4.51198	–4.4975	–1.70907
PDAC88	PDAC	–3.24846	–1.57605	–2.59919	–5.77902	–1.34579

Supplementary Table 10. Clinicopathologic Characteristics of CA19-9–Negative Cases Plasma Samples From the Final Performance Evaluation Cohorts

Variables	CA19-9–negative cases, n (%)		*P* value
	Patients with PDAC (n = 20)	Healthy controls (n = 41)	
Age, *y*, mean ± SD	70.3 ± 7.5	42.7 ± 12.3	<.01[a]
Sex, n (%)			.397[b]
Male	9 (45.0)	13 (31.7.0)	
Female	11 (55.0)	28 (68.3)	
Race, n (%)			.002[c]
White	11 (55.0)	38 (92.7)	
Black	7 (35.0)	2 (4.9)	
Unknown	2 (10.0)	1 (2.4)	
TNM stage, n (%)[d]			—
1 and 2	16 (80.0)	NA	
3 and 4	4 (20.0)	NA	

[a] *t* test.
[b] Fisher exact test.
[c] Pearson χ^2 test.
[d] TNM stage was based on *AJCC Cancer Staging Manual*, 8th edition.[16]